Formation of submarine lava channel textures: Insights from laboratory simulations

W. Brent Garry,[1] Tracy K. P. Gregg,[1] S. Adam Soule,[2] and Daniel J. Fornari[2]

Received 25 April 2005; revised 23 August 2005; accepted 13 December 2005; published 28 March 2006.

[1] Laboratory simulations using polyethylene glycol (PEG) extruded at a constant rate and temperature into a tank with a uniform basal slope and filled with a cold sucrose solution generate channels that are defined by stationary levees and mobile flow interiors. These laboratory channels consistently display the following surface textures in the channel: smooth, folded, lineated, and chaotic. In the simulations, we can observe specific local conditions including flow rate, position within the channel, and time that combine to develop each texture. The textures in PEG flows form due to relative differences in shear forces between the PEG crust and the underlying liquid wax. Minimal shear forces form smooth crust, whereas folded crust forms when the shear is sufficiently high to cause ductile deformation. Brittle deformation of solid PEG creates a chaotic texture, and lineated crust results from shear forces along the channel-levee margin. We observe similar textures in submarine lava channels with sources at or near the Axial Summit Trough of the East Pacific Rise between 9° and 10°N. We mapped the surface textures of nine submarine lava channels using high-resolution digital images collected during camera tows. These textural maps, along with observations of the formation of similar features in analog flows, reveal important information about the mechanisms occurring across the channel during emplacement, including relative flow velocity and shear stress.

Citation: Garry, W. B., T. K. P. Gregg, S. A. Soule, and D. J. Fornari (2006), Formation of submarine lava channel textures: Insights from laboratory simulations, *J. Geophys. Res.*, *111*, B03104, doi:10.1029/2005JB003796.

1. Introduction

[2] Lava channels have been documented in subaerial flows with various compositions [e.g., *Macdonald*, 1953; *Dawson et al.*, 1990; *Harris et al.*, 2004], in submarine lavas [e.g., *Fornari et al.*, 1985], on the Moon [*Hulme and Fielder*, 1977], Mars [e.g., *Mouginis-Mark et al.*, 1992], Venus [e.g., *Baker et al.*, 1992], and Io [e.g., *Williams et al.*, 2001]. Channels are a thermally and mechanically efficient means of transporting lava, and their presence at fast and superfast spreading centers [*Fornari et al.*, 1998, 2004; *Sakimoto and Gregg*, 2001; *Cormier et al.*, 2003; *White et al.*, 2000, 2002; *Soule et al.*, 2005] has implications for eruption styles as well as the construction of oceanic crust. Submarine lava flow surface morphology has been used to interpret the dynamics of flow emplacement [e.g., *Gregg and Fink*, 1995; *Gregg and Chadwick*, 1996; *Soule et al.*, 2005]. Here, we examine submarine lava channels observed on the East Pacific Rise (EPR) between 9°28′N and 9°51′N (Figure 1), and compare their detailed surface textures with similar textures produced during controlled laboratory simulations in which polyethylene glycol (PEG) wax is extruded to generate a channel [e.g., *Fink and Griffiths*, 1990; *Griffiths and Fink*, 1992; *Gregg and Fink*, 2000]. We focus on the specific textures observed within lava channels along the Northern EPR rather than the more general problem of submarine channel formation. We address how these textures form and what the distribution of these textures across a channel reveals about the flow dynamics occurring within the channel during emplacement.

[3] *Fink and Griffiths* [1990] and *Gregg and Fink* [2000] used PEG to simulate lava flow emplacement, and concluded that high effusion rates, high eruption temperatures, low viscosities, low cooling rates and high underlying slopes favor the generation of lava channels over other possible flow morphologies. *Fink and Griffiths* [1990] and *Griffiths and Fink* [1992] quantitatively described morphologies in simulated PEG flows based on solidification rate of the crust versus the downstream advection of heat. This ratio is described by the dimensionless number, $\Psi = t_s/t_a$, where t_s is time of solidification and t_a is time of advection. For point source eruptions of a viscous flow, Ψ is described as:

$$\Psi = t_s / \left[(\nu_c / g')^{3/4} Q^{-1/4} \right] \quad (1)$$

where ν_c is the kinematic viscosity of the crust, g' is reduced gravity ($g' = g\,[\rho_l - \rho_w]/\rho_l$), and Q is volumetric effusion rate from the vent (Table 1) [*Gregg and Fink*, 2000]. The

[1]Department of Geology, State University of New York at Buffalo, Buffalo, New York, USA.
[2]Woods Hole Oceanographic Institution, Department of Geology and Geophysics, Woods Hole, Massachusetts, USA.

0148-0227/06/2005JB003796$09.00

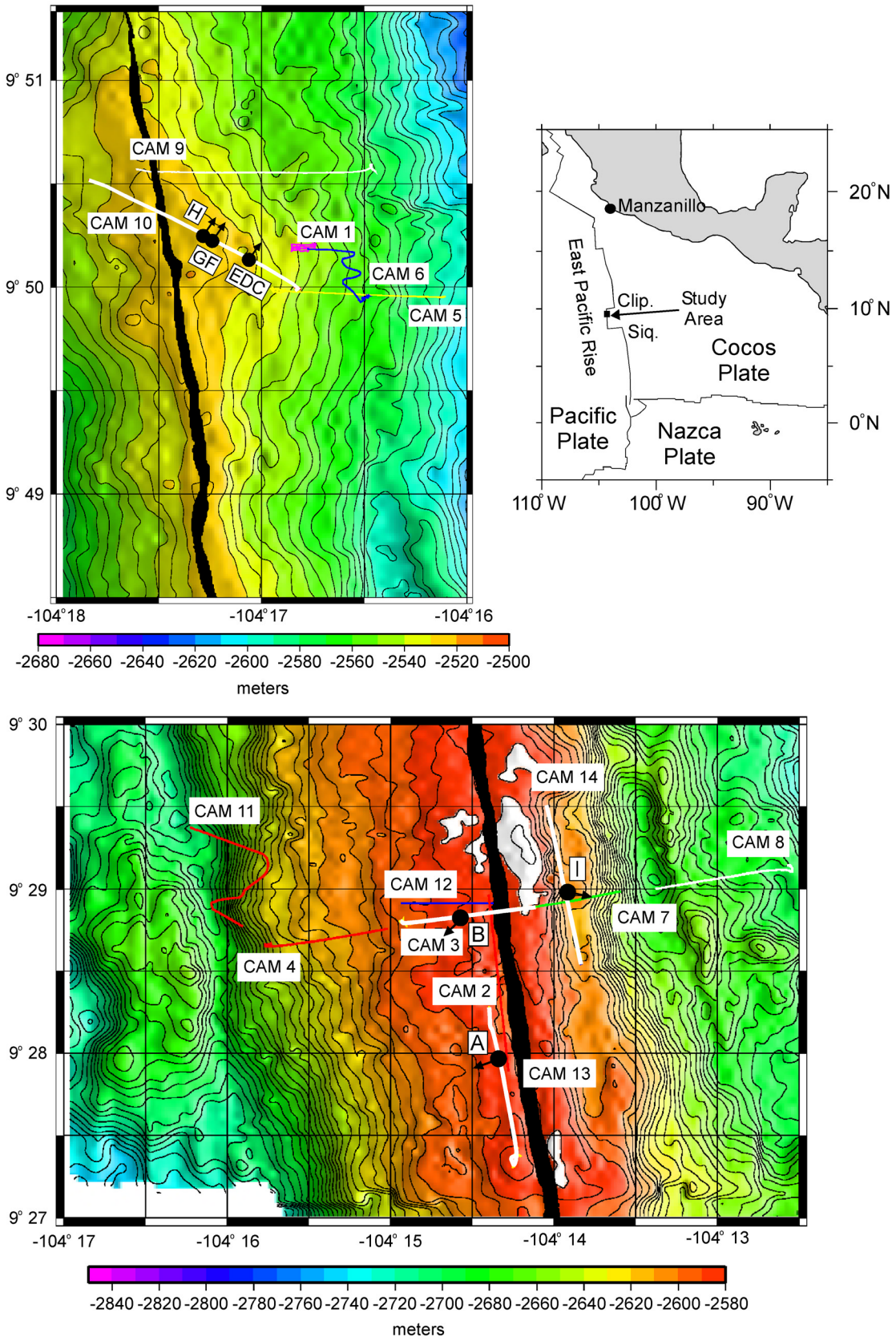
9° 51
9° 50
9° 49
CAM 9
CAM 10
H
GF
EDC
CAM 1
CAM 6
CAM 5
-104°18
-104°17
-104°16
-2680 -2660 -2640 -2620 -2600 -2580 -2560 -2540 -2520 -2500
meters
Manzanillo
20°N
10°N
0°N
East Pacific Rise
Clip.
Siq.
Study Area
Cocos Plate
Pacific Plate
Nazca Plate
110° W
100° W
90° W
9° 30
9° 29
9° 28
9° 27
CAM 14
CAM 11
CAM 8
I
CAM 12
CAM 7
B
CAM 3
CAM 4
CAM 2
A
CAM 13
-104° 17
-104° 16
-104° 15
-104° 14
-104° 13
-2840 -2820 -2800 -2780 -2760 -2740 -2720 -2700 -2680 -2660 -2640 -2620 -2600 -2580
meters

Figure 1

Table 1. Notation

Parameter	Definition	Unit
g	gravity	m s^{-2}
g'	reduced gravity	m s^{-2}
Q	volumetric effusion rate	m^3 s^{-1}
q	linear effusion rate	(m^2 s^{-1}) m^{-1}
ρ_a	density (ambient)	kg m^{-3}
ρ_l	density (lava)	kg m^{-3}
t_s	timescale for solidification	s
t_a	timescale for heat advection	s
ν_c	kinematic viscosity (crust)	m^2 s^{-1}

relation for line source eruptions is given by [*Griffiths and Fink*, 1992]

$$\Psi = (g\Delta\rho/\rho_l\nu_c)^{2/3}q^{1/3}t_s \quad (2)$$

where q is linear effusion rate (m^2/s/m) or square meters per second per meter length of fissure. Though axial eruptions are dominantly line source eruptions along the axis [*Haymon et al.*, 1991; *Gregg et al.*, 1996; *Fornari et al.*, 1998], individual channels can be accurately modeled as point source eruptions [*Gregg and Fink*, 2000].

[4] *Gregg and Fink* [2000] determined ranges of Ψ for morphologies in PEG flows on 10° slopes: pillows $\Psi < 1$, rifts $1 < \Psi < 7$, folds $7 < \Psi < 22$, and levees $\Psi \geq 22$. The minimum Ψ values for levee formation decrease as slope increases, with a major transition between 30° ($\Psi > 21$) and 40° ($\Psi > 9$) [*Gregg and Fink*, 2000]. The ranges of Ψ values determined in the laboratory for specific flow types have been repeatedly shown to correlate well with Ψ values calculated for natural lava flows that show the same general flow characteristics [*Fink and Griffiths*, 1990; *Griffiths and Fink*, 1992, 1997; *Gregg and Fink*, 1995, 1996, 2000].

[5] Submarine lava channels have been documented in a variety of volcano-tectonic settings, including: the Puna Ridge, Kilauea Volcano, Hawaii [*Gregg and Smith*, 2003]; near-ridge seamounts in the Pacific [*Fornari et al.*, 1985] and in the Mid-Atlantic Ridge [*Smith and Cann*, 1999]; and at fast and superfast spreading centers [*Gregg et al.*, 1996; *White et al.*, 2000, 2002; *Cormier et al.*, 2003; *Fornari et al.*, 2004; *Soule et al.*, 2005]. The lava channels presented in our study are emplaced along the Northern EPR (Figure 1). *Soule et al.* [2005] found that channeled lava flows are common along this segment of the EPR and described their origins, and their connection to crustal growth and ridge geometry along the EPR. This paper complements the *Soule et al.* [2005] study by looking at the detailed distribution of the surface textures within submarine lava channels to better understand flow dynamics inside a channel during emplacement. Using careful characterization of the distribution of surface textures found within PEG channeled flows and submarine lava channels, we are able to infer the processes involved during the emplacement of these textures along the EPR, thereby providing insight into the dynamics of individual mid-ocean ridge eruptions.

2. Simulated Channels

2.1. Data

[6] Using laboratory simulations we can observe and measure the processes that form channel textures in a controlled environment. PEG has been successfully used to simulate basaltic lava flows in subaerial, submarine, and extraterrestrial environments [*Fink and Griffiths*, 1990; *Griffiths and Fink*, 1992; *Gregg and Fink*, 1995, 1996; *Blake and Bruno*, 2000]. In our simulations, warm (22°–26°C; solidification temperature is ~20°C) PEG is pumped at a constant effusion rate (5.0–6.5 mL/s) into a chilled (7°–12°C) sucrose solution through a 1-cm-diameter vent at the upslope end of a floor in a Plexiglas tank (71 cm long, 28 cm wide) set at a specified slope (8°–10°) in what we refer to as the ''effusion'' stage of the flow. Though slopes at the EPR crest are commonly 4°–6° [*Fornari et al.*, 1998, 2004; *Soule et al.*, 2005] (e.g., Figure 1), simulated channels are more reliably formed on slopes of 8°–10° with our laboratory setup. *Gregg and Fink* [2000] demonstrated that processes that occur in the development of simulated channels are still applicable to submarine channels formed on underlying slopes ≤10°. The tank floor is covered with a steel mesh with wire spacing of 0.40 cm^2. The mesh provides a nonslip surface; without the mesh, PEG slides along the flow base [cf. *Fink and Griffiths*, 1990; *Gregg and Fink*, 2000]. Total eruption volumes were constrained to <2000 mL of wax and durations to <300 s, due to tank dimensions.

[7] The phase we define as ''drainout'' begins when the PEG pump is turned off, the vent is plugged, and the remaining wax continues to flow downstream after effusion has ceased. This is different from ''drainback,'' where lava flows back into the source vent after the eruption has ceased [*Gregg et al.*, 1996]. Flow widths are typically >20 cm, but maximum flow dimensions are constrained by the width and length of the tank. Parameters and dimensions for individual flows generated for this study are listed in Table 2.

2.2. Laboratory Surface Textures

[8] We have classified four textures that form in simulated flows as smooth, lineated, folded, and lobate (Figure 2), terms that are consistent with similar submarine lava flow textures (Figure 3) [*Griffiths and Fink*, 1992; *Gregg and Fink*, 1995]. Crust that is flat, with little to no surface relief, is defined as smooth. We commonly observe the formation of smooth crust proximal to the vent. Cusps and folds with their axes parallel to the flow direction are preserved in solidified PEG at the channel-levee margins and are characteristic of lineated crust observed in the

Figure 1. Locations of submarine lava channels (circles) imaged in camera tow surveys along the track plots of the 14 camera tow surveys conducted along the EPR during cruise AT 07-04. Arrows indicate flow direction within channel. Letters refer to individual channels mapped in this study. See Figure 11 and Table 3. Bathymetry data are obtained by multibeam sonar. Contour interval is 5 m. Axial Summit Trough is blackened for reference; outline is from 1989 Argo survey [*Haymon et al.*, 1991; *Fornari et al.*, 1998].

Table 2. Eruption Parameters for Simulated Channels

Flow	Slope	$T_{solution}$, °C	$\rho_{solution}$, g/cm^3	T_{wax}, °C	Q, mL/s	Volume,[a] mL	Duration,[b] s	Ψ
BG-49	8	9.00	1.1130	24	6.37	1510	237	15.2
BG-59	10	7.50	1.1160	24	6.52	1473	226	8.1
BG-63	10	9.50	1.1075	23	6.21	1068	172	17.0
BG-65	10	9.00	1.1175	24	5.81	1103	190	9.2
BG-67	10	10.00	1.1100	23	5.87	1473	251	17.1
BG-69	8	10.00	1.1135	24	6.16	1552	252	19.1
BG-71	8	12.00	1.1175	24	5.96	1687	283	24.0
BG-72	8	11.00	1.1135	25	6.03	1634	271	34.2
BG-74	8	12.00	1.1160	24	6.11	1593	261	29.3
BG-75	8	11.00	1.1150	24	5.85	1047	179	22.4

[a]Volumes calculated by multiplying effusion rate and duration.
[b]Duration calculated from initial effusion from vent to the moment wax is cut off.

simulated flows. These patches of lineated PEG are typically narrow (1–2 cm wide) relative to total channel width and elongate in the direction of flow. Folded crust forms folds that resemble subaerial pahoehoe ropes with fold axes perpendicular to flow direction. Lobate crust has an undulating, bulbous surface, similar to subaerial pahoehoe toes and forms along the flow margins, and comprises levees.

[9] We use the term "chaotic" for PEG textures analogous to jumbled textures on submarine lava flows [e.g., *Perfit and Chadwick*, 1998]. We interpret regions of solid clumps of wax mixed with liquid PEG or disrupted crust as chaotic, because a coherent, recognizable morphology does not form. Two mapping units are specific for the simulation morphology: "mesh" and "liquid." Sections of the channel where there is no overlying liquid or solid PEG are mapped as mesh, referring to the wire screen on the floor of the tank that is visible. Some wax has not yet solidified in the final images used for mapping, and is therefore mapped as liquid. Although the formation of circular "rosettes" of PEG crust within shear zones at the channel margins have been reported [*Griffiths et al.*, 2003], we did not observe them in our simulations. The PEG "rosettes" appear to resemble lava coils observed in submarine flows (Figure 3g) [e.g., *Lonsdale*, 1977; *Gregg and Fink*, 2000].

2.3. Emplacement of a PEG Channel

[10] A sequence of four images and texture maps in Figure 4 illustrate the evolution of a typical PEG channel from initial levee formation to final, solidified morphology and exemplified by simulation BG-75. At the start of the simulation, PEG spreads axisymmetrically from the vent. Lobate levees are established ~30 s into the simulation, at the margins of the PEG flow, beginning the channel-forming process. Levee widths stabilize after ~120 s and are typically narrow (<2 cm wide), but can fluctuate in width downstream (0.5–4.0 cm) and may extend >30 cm from the vent. Observations indicate that once levee widths have stabilized, and reached a critical width, additional growth of the levee inward toward the channel center is limited during the remainder of the effusion and drainout stages. Levee thicknesses range from 0.5 to 2.0 cm and mimic the maximum depth of the PEG flow proximal to the vent. In cross section, levees exhibit a concave morphology, with the outer portion of the levees composed of lobate textures and the inner portion composed of a thin overhang, ≤3 cm wide, of lineated or chaotic crust (Figures 5a and 5b). Measurements of levee morphology show that, at any given cross section along the channel, liquid material flowing beneath the overhang portions of the levees makes up 10–20% of total liquid material flowing within the channel. After the active effusion stage, and during drainout, crust forming within the channel typically subsides with the level of liquid wax, leaving the levees free-standing (Figures 5a and 5b). We refer to the levees with respect to an observer looking downstream, where the left levee is located at the top and the right levee is located at the bottom of each image in Figure 4.

[11] After 70 s, wax in Figure 4a has flowed a distance of 26 cm from the vent, but the levees do not extend the entire length of the flow. The left levee extends 10 cm whereas the right levee extends 18 cm downstream. The levees are wider at the vent and narrow downstream. A crust does not form on the liquid wax in the channel until it reaches ~12 cm from the vent where a single train of folded crust originates. A distinct, narrow zone of crust-free, liquid PEG divides the fold train from the right levee. Lineated textures form along the levees near the vent.

[12] We must note that folded crust in PEG channels constructs a fairly continuous structure that we refer to as a "fold train." The location in the channel where folded crust begins to form remains at a set distance from the vent for the duration of the experiment: 8° slope (≤28 cm) and 10° slope (4–16 cm). Figure 4 shows a single "fold train" forming in the channel, but we have observed as many as three narrow, parallel fold trains form across the channel and each fold train maintains a relatively constant width (Figure 6a). Fold trains are separated from each other and the channel-levee margins by crust-free shear zones (Figure 6b). Downstream, fold trains are disrupted into slabs, which overlap and rotate, but the folded texture is still recognizable. We have not observed folded crust to form directly adjacent to the channel-levee margin.

[13] After 134 s, the levees reach >20 cm on either side of the flow, which has advanced 46 cm from the vent (Figure 4b). Surface folds still form ~12 cm from the vent and the channel area proximal to this point remains crust-free. The fold train is 36 cm long and is separated from the margins by a liquid shear zone. Lineated crust begins to solidify on the right margin of the channel within a shear zone. Downstream, past the end of the levees, "chaotic" textured crust characterizes the flow margins.

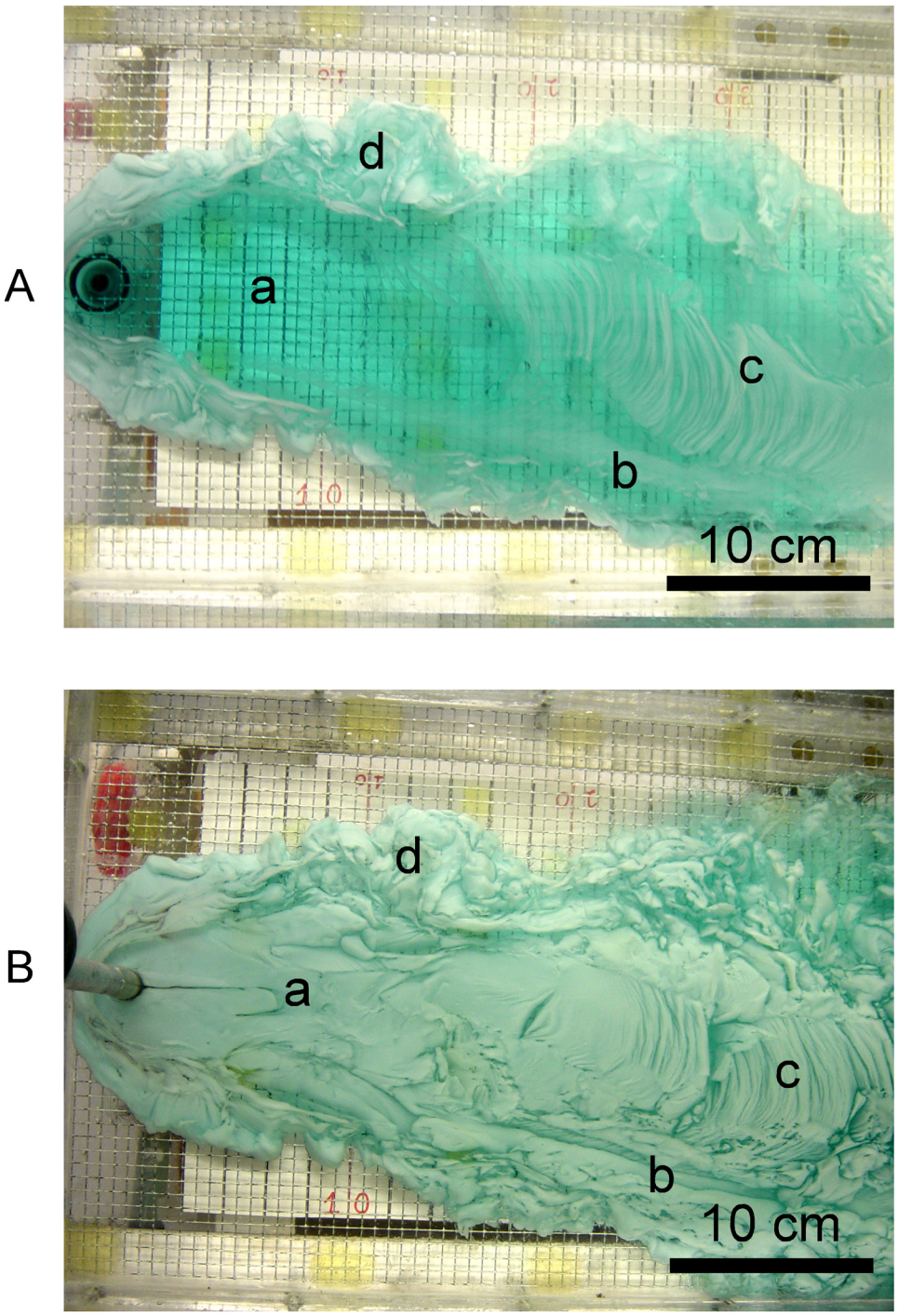

Figure 2. (a) Surface morphology of a PEG channel during effusion. (b) Final flow morphology of the same PEG channel after drain out. Lighter toned material is solidified PEG; darker toned material is liquid PEG. Corresponding locations of final surface textures to the same areas during emplacement are marked on both images: a, smooth; b, lineated; c, folded; and d, lobate. The vent is visible at the far left and the flow direction is toward the right. Images are from simulation BG-75.

[14] After 180 s, the vent was plugged, marking the beginning of the drainout process. The flow reached a length of 70 cm after 198 s (Figure 4c). A liquid, crust-free channel is still present near the vent, but smooth crust now forms ~12 cm from the vent instead of folded crust. The smooth crust is attached to the trailing edge of the fold train. The fold train grew to >40 cm in length, despite having been broken, rotated, and overlapped in a few areas. A narrow band of lineated crust continues to form in the shear zone on the right side of the flow, while the left

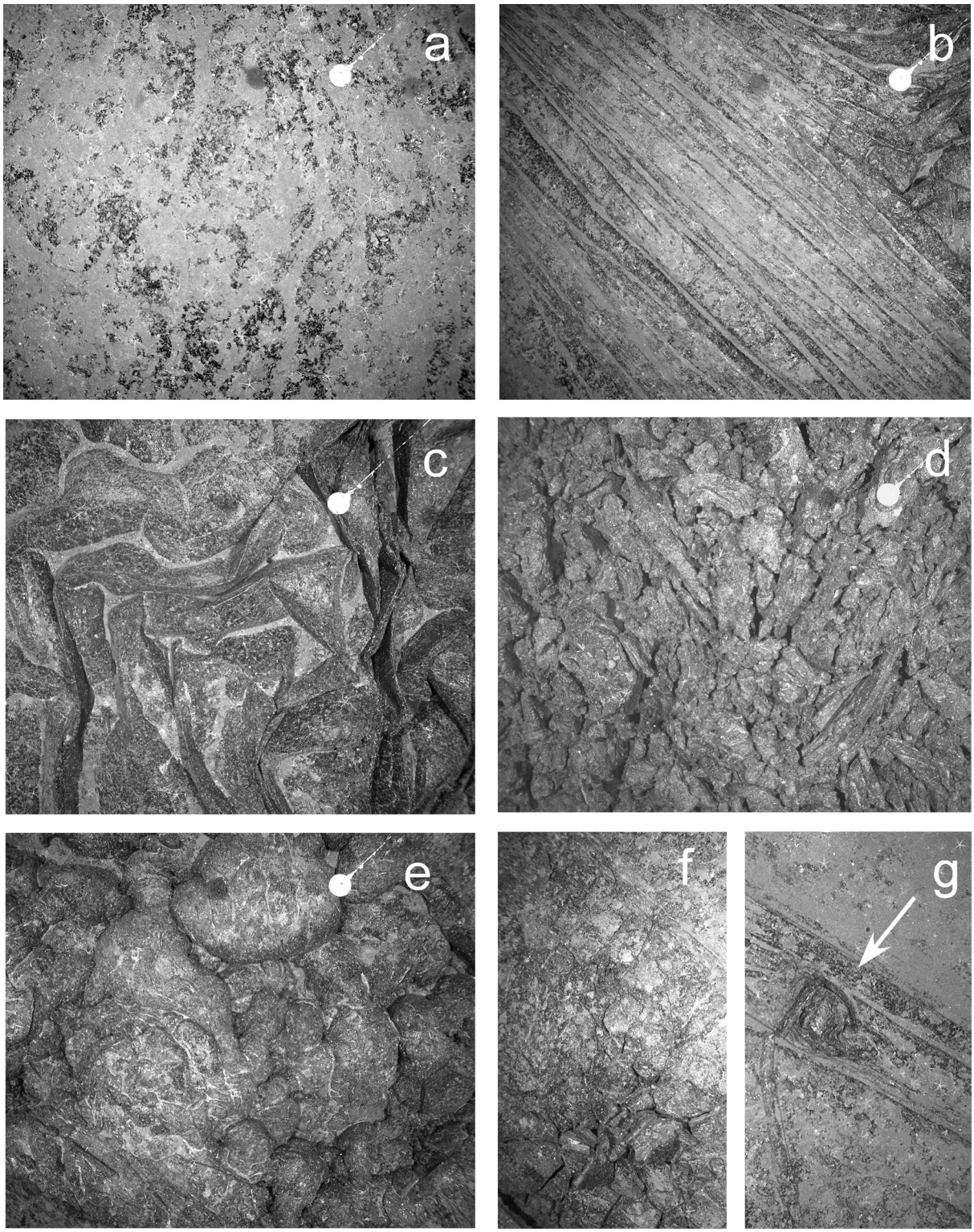

Figure 3. Examples of surface textures and structures mapped in submarine lava channels: (a) smooth, (b) lineated, (c) folded, (d) jumbled, (e) lobate, (f) jigsaw, and (g) lava coil. Field of view is ~5 m across Figures 3a–3e and ~2 m across for Figures 3f and 3g. All images are collected from EPR cruise AT 07—04.

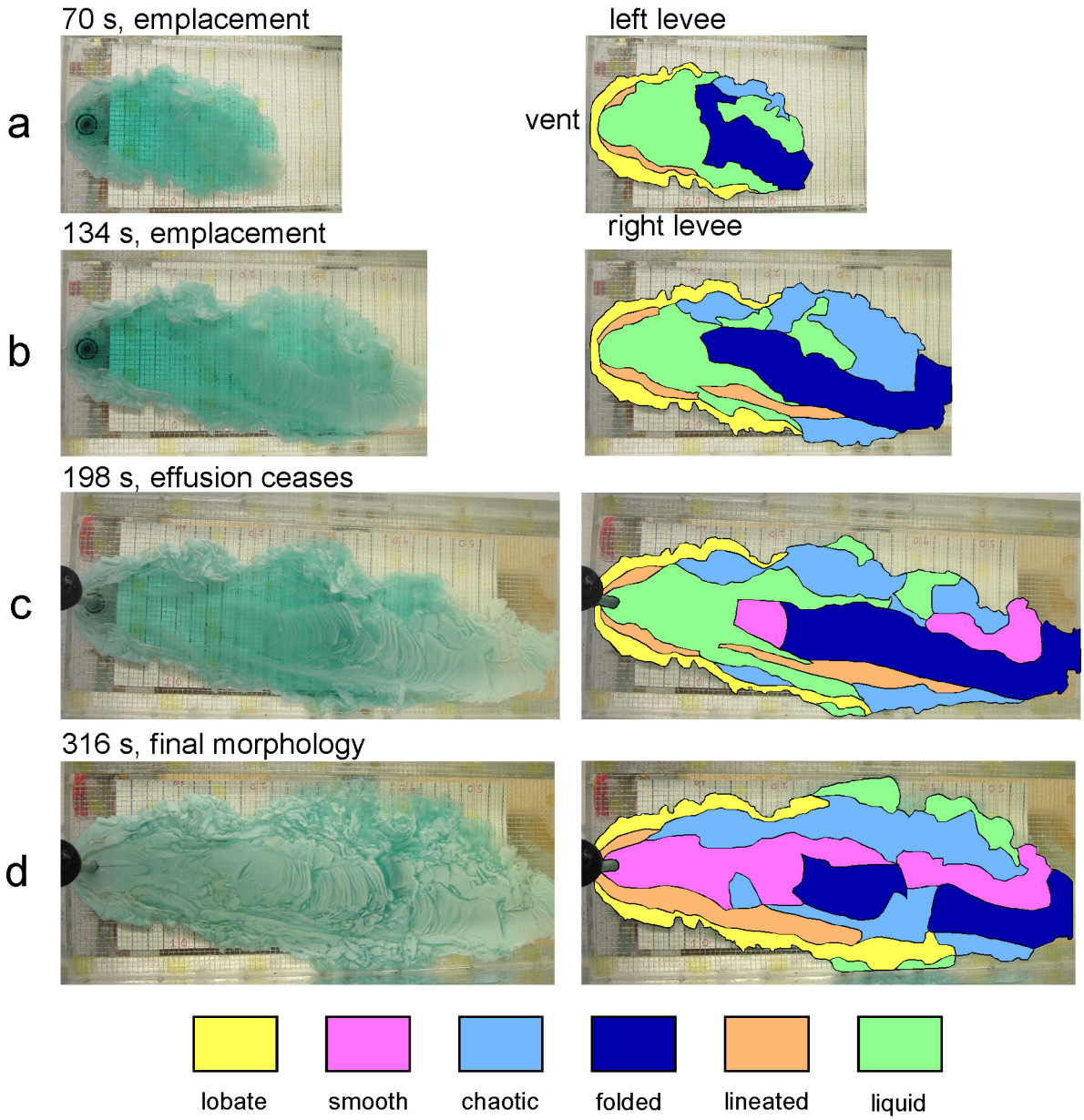

Figure 4. Progression of simulation BG-75 with time. (left) Top view still images and (right) corresponding texture maps. Times given are total seconds after start of simulation. Underlying slope is 10°, and flow direction is to the right. The PEG is flowing over a wire mesh, and dark lines perpendicular to flow are spaced at 2-cm intervals.

side of the flow is dominated by liquid and chaotic textured crust.

[15] The surface of the remaining PEG in the channel solidifies after 316 s, although some liquid wax remains on the downstream edges of the flow and beneath the crust (Figure 4d). Smooth crust forms in the central part of the channel where the liquid area was located in the previous stages. Chaotic crust separates the central train of folded and smooth crust from the left channel margin. The shear zone on the right side of the flow is now a narrow band of lineated crust. The lack of lineated crust along the left channel-levee margin may be due to the asymmetrical outline of the levee, where the right levee is fairly linear, and the left levee undulates (Figure 4d). Note that there is no observed deformity in the tank floor to cause this asymmetry.

2.4. PEG Surface Texture Distribution

[16] We mapped the final surface textures of 10 simulated channels, 4 of which are shown in Figure 7. In the following description of the spatial and temporal evolution of surface textures observed in the simulated flows, we have defined the channel as the area of the flow bound by the levees, because that corresponds with what we can clearly identify in the submarine flows. We have only analyzed and reported coverage of the crust in the channel up to the extent of the longest levee for purposes of comparison with available submarine data.

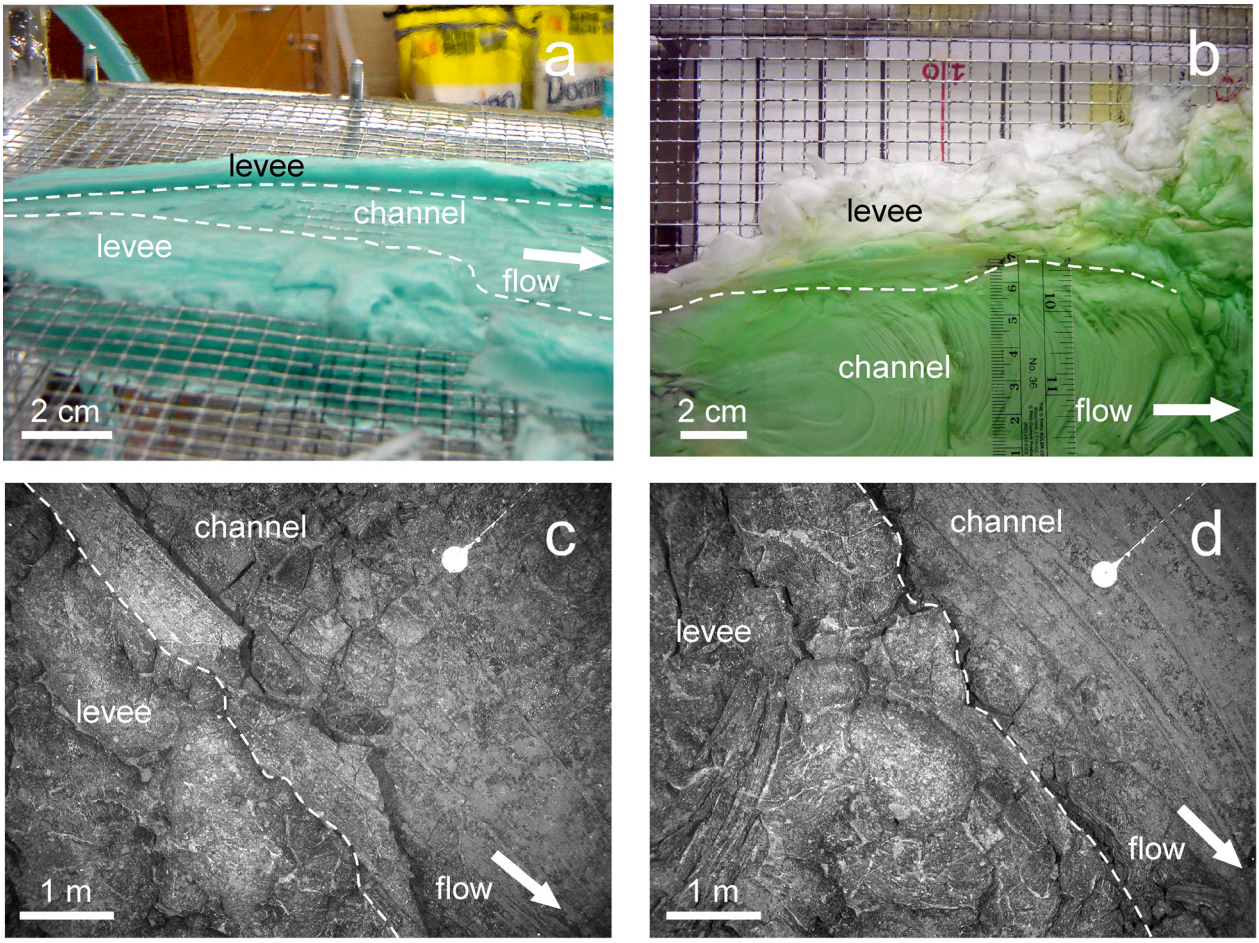

Figure 5. Channel-levee margins for two PEG channels (Figures 5a and 5b) and two submarine channels (Figures 5c and 5d). Dashed line marks the channel-levee margin. Arrows mark flow directions. The channel crust in each image rests at a lower level with respect to the levee crust. (a) An oblique view of the remnant crust of a PEG channel after the wax as drained from the channel. (b) Top view of a simulated channel. The concave morphology of the left levee is revealed by a ruler that extends 3 cm beneath the overhang portion of the left levee. (c) Lineated crust from the submarine channel is still attached to the lobate levee crust. (d) Sharp transition in textures at the channel-levee margin, from lobate to lineated.

[17] We consistently observe specific crust morphologies forming at particular locations within a channel (Figures 2 and 7) and in specific temporal sequences (Figure 4), although the surface coverage by a particular texture may vary greatly between flows (Figures 7 and 8). In all simulated channels, we observe that (1) lobate crust forms the levees; (2) folded PEG is located in the central part of the channel; (3) smooth-textured crust forms proximal to the vent; (4) lineated crust or narrow patches of smooth crust are located adjacent to the levees and at the along-flow margins of fold trains; and (5) chaotic crust is distributed along the channel levee margins and beyond the downstream end of the levees.

[18] The most abundant textures preserved between the levees of the final flow morphology are smooth and chaotic, which combine for 59% of the total area mapped for PEG channels (Figure 8a). Simulated channels on 8° slopes tend to have a higher percentage of coverage by smooth textures than do those on 10° slopes (Figure 8b). Smooth crust covers 33–64% of the channel for PEG simulations formed on 8° slopes, whereas coverage in channels on 10° slopes varies from 8 to 34% (Figure 8b). Folded crust covers 13% of the mapped channels. For a given flow, the fraction of coverage by folded crust preserved within the defined channel is not always representative of the folded crust formed during the emplacement or preserved beyond the defined channel. Channels on slopes of 10° have a higher fraction (11–40%) of folded crust preserved in the channel than do those formed on 8° slopes (0–19%) (Figure 8b). Lineated crust is observed to form adjacent to channel-levee margins and only accounts for 9% of the textures mapped in the PEG channels (Figure 8a). Channels formed on slopes of 10° have a higher percentage of lineated crust preserved (Figure 8b). The three experiments (BG-71, BG-72, BG-74) with the highest Ψ–values ($24.0 \leq \Psi \leq 34.2$) have the least

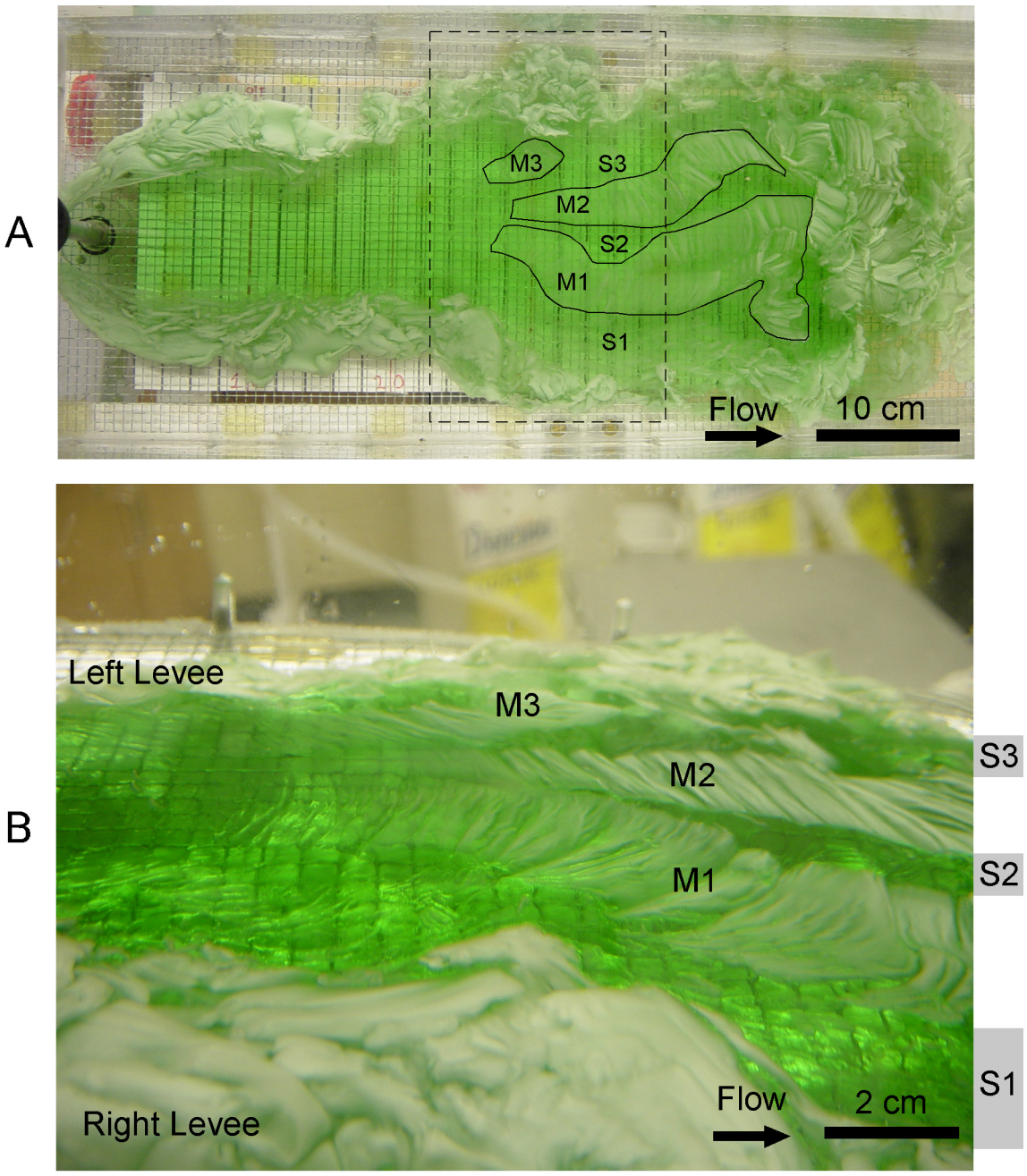

Figure 6. Three fold trains of mobile, folded crust separated by shear zones in a PEG channel. (a) Top down view of PEG channel BG-74 (Table 2). Vent is located at the left, and flow is to the right of the image. Darker colored PEG is liquid, while lighter colored PEG is solid. The trains of mobile crust within channel are outlined by a solid line and indicated by M1, M2, and M3. Shear zones are indicated by S1, S2, and S3. The dashed box outlines the field of view in the lower image. (b) An enlarged, oblique view of the channel surface showing spatial distribution of the three fold trains separated by the three shear zones.

amount of folded and lineated crust preserved within the channel.

3. Submarine Channels

3.1. Data Acquisition

[19] Data for submarine lava channels used in this project were obtained during R/V *Atlantis* cruise AT 07-04 in 2000 [*Schouten et al.*, 2002; *Fornari et al.*, 2004]. Several near-bottom survey instruments were used to map the EPR between 9° and 10°N (Figure 1). These include a 120-kHz side-scan sonar (DSL-120A [e.g., *Scheirer et al.*, 2000]) with ~2 m pixel resolution; and the Autonomous Benthic Explorer (ABE) [*Yoerger et al.*, 1998] which collected near-bottom bathymetry to produce bathymetric maps with ~5 m horizontal and 1 m vertical resolution

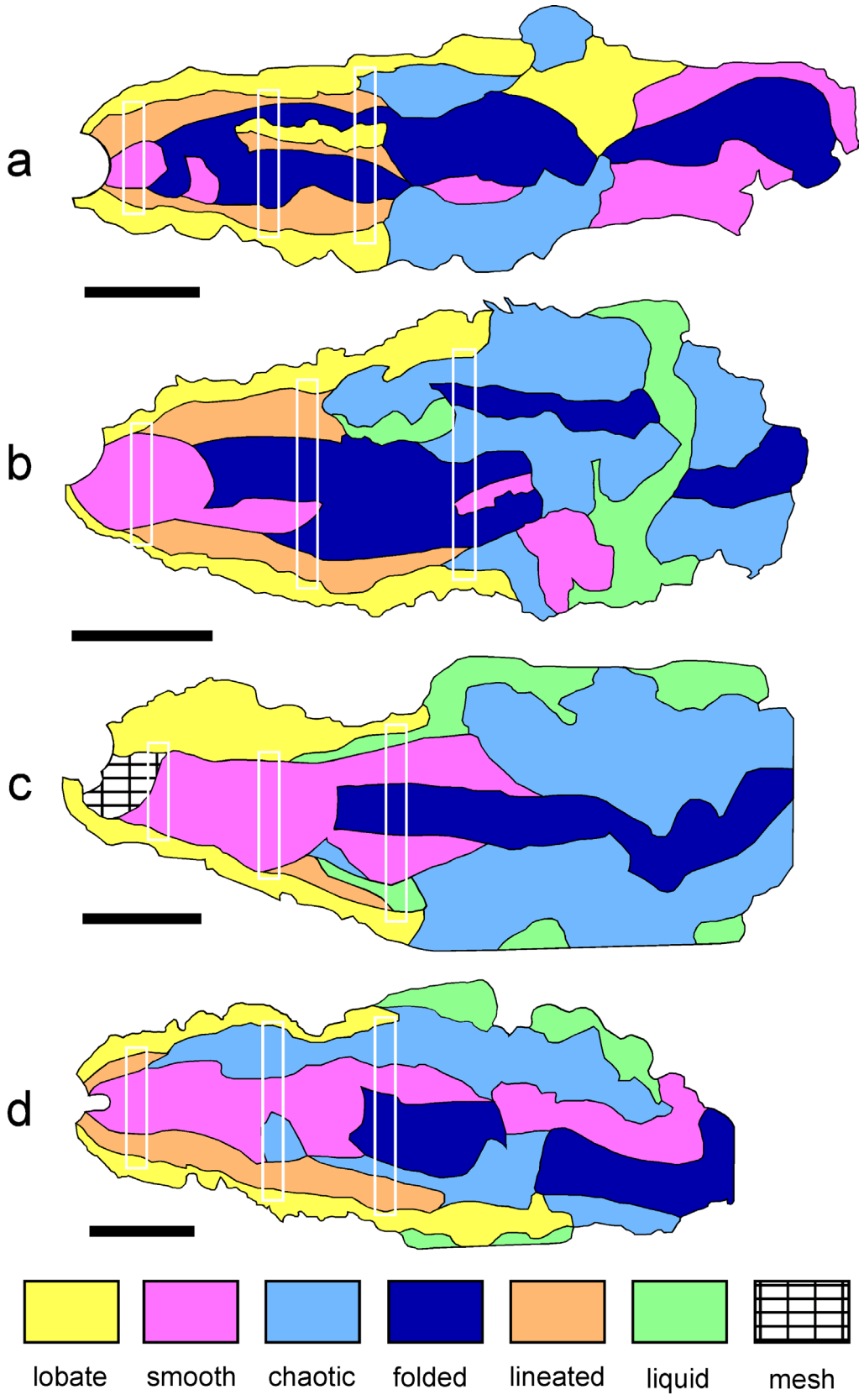

Figure 7. Texture maps of the final drained morphology of four simulated channeled flows. The maps are from the following simulations: (a) BG-59, (b) BG-63, (c) BG-67, and (d) BG-75. Each scale bar represents 10 cm. Direction of flow is from left to right. Straight edges are where the flow has encountered the tank wall. The white boxes represent the sections of channel that were analyzed for fraction of coverage by textures at different intervals from the vent presented in Figure 14.

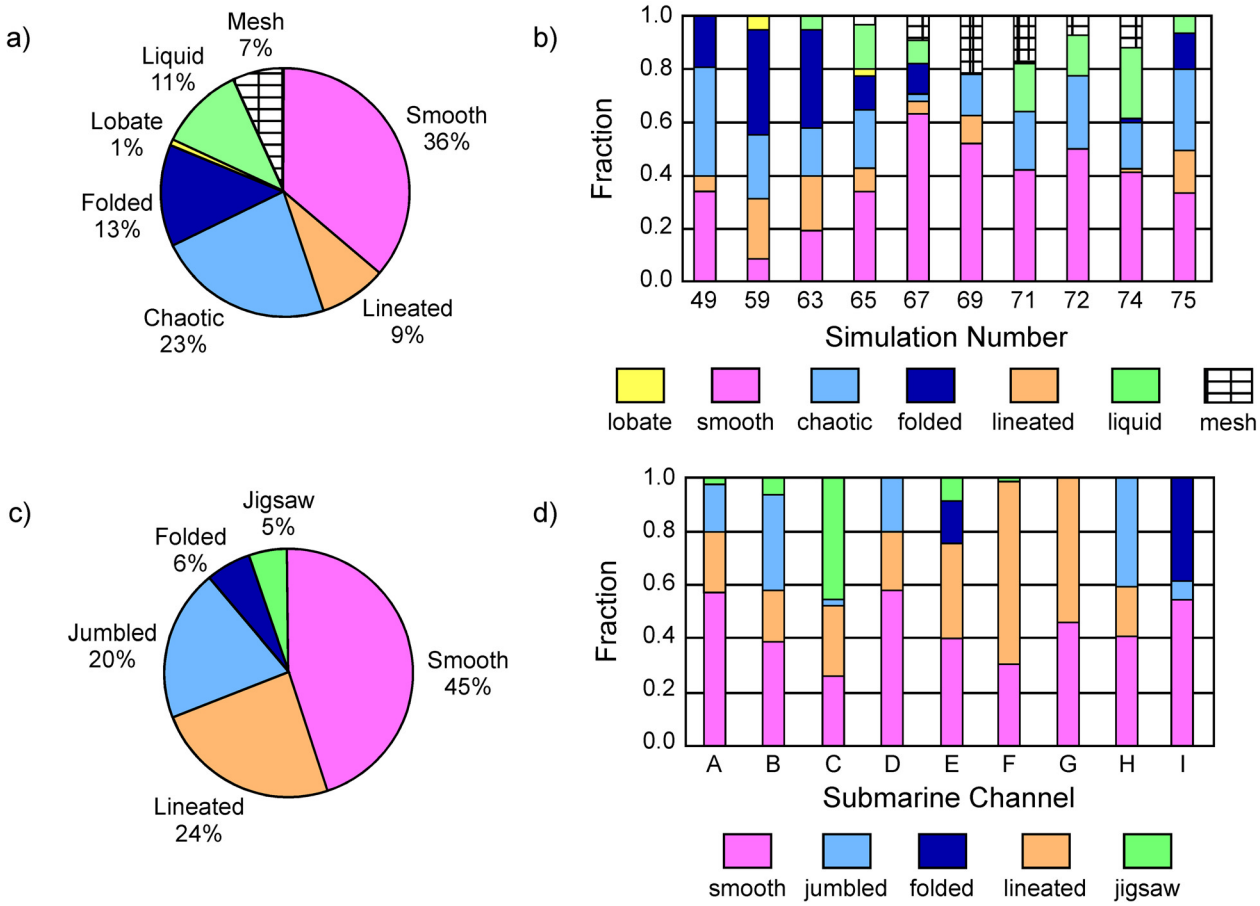

Figure 8. (a) Percent coverage by each texture for all simulated channels (n = 10). (b) Total fraction of coverage by each texture in the simulated channels. Lobate levees and downstream textures extending beyond end of defined channel are not included. (c) Percent coverage by each texture totaled for all submarine channels, not including lobate levees (n = 9). (d) Fraction of coverage by each texture for individual submarine channels. These represent partial sections of individual channels and do not reflect the downstream change in texture of a single channel or entire individual channels.

[*Schouten et al.*, 2002; *Fornari et al.*, 2004]. In addition, a deep-sea digital towed camera was used to collect seafloor imagery from an altitude of ~5 m with centimeter-scale image resolution [*Fornari*, 2003] to provide photographs of submarine channel morphology. Traverses were usually ~1–2 km in length and were planned using the DSL-120A sonar images (Figure 9) and navigated by acoustic transponders [*Schouten et al.*, 2002]. The digital camera recorded still images at 15 s intervals, each covering an area of ~30 m^2 at 2048 × 1536 pixels per snapshot. Overall, 14 tow camera surveys were conducted (Figure 1), collecting >8,000 images of on- and off-axis lava flows. The lavas here are known to be basalts [e.g., *Perfit and Chadwick*, 1998].

3.2. Identification, Locations, and Dimensions of Submarine Lava Channels

[20] Submarine lobate lavas are believed to form at lower flow velocities than those needed to produce lineated and folded textures preserved within the submarine channel interior [*Griffiths and Fink*, 1992; *Gregg and Fink*, 1995]. We interpret zones of lineated, smooth, and folded crust bound by levees of more bulbous, lobate crust as submarine lava channels (Figure 10). Hereafter, the term "channel," when used in the submarine context, refers to the material found between the bounding lobate levees.

[21] We have identified nine submarine lava channels (A through I) within six mosaics of images from four different camera tows. All channels identified and mapped for this study are located within 1 km of the Axial Summit Trough (AST) [*Haymon et al.*, 1991; *Fornari et al.*, 1998, 2004, also The axial summit trough and crest of the East Pacific Rise 9°09′–59′N: New insights on submarine eruption and transport processes based on DSL-120A sidescan and ABE sonar surveys, manuscript in preparation, 2005]. Local flow directions, determined by orienting the mosaics to the camera tow traverse, are inferred to be dominantly oblique to the trend of the AST (Figure 1). Locations of the submarine channels along the camera tow traverse coincide with the dark patches observed in the DSL-120A data (Figure 9). These dark patches are interpreted to be channeled lava flows based on the smooth surface indicated by their low acoustic reflectivity [*Fornari et al.*, 2004; *Soule et al.*, 2005]. The lava channels are considered to be a type of

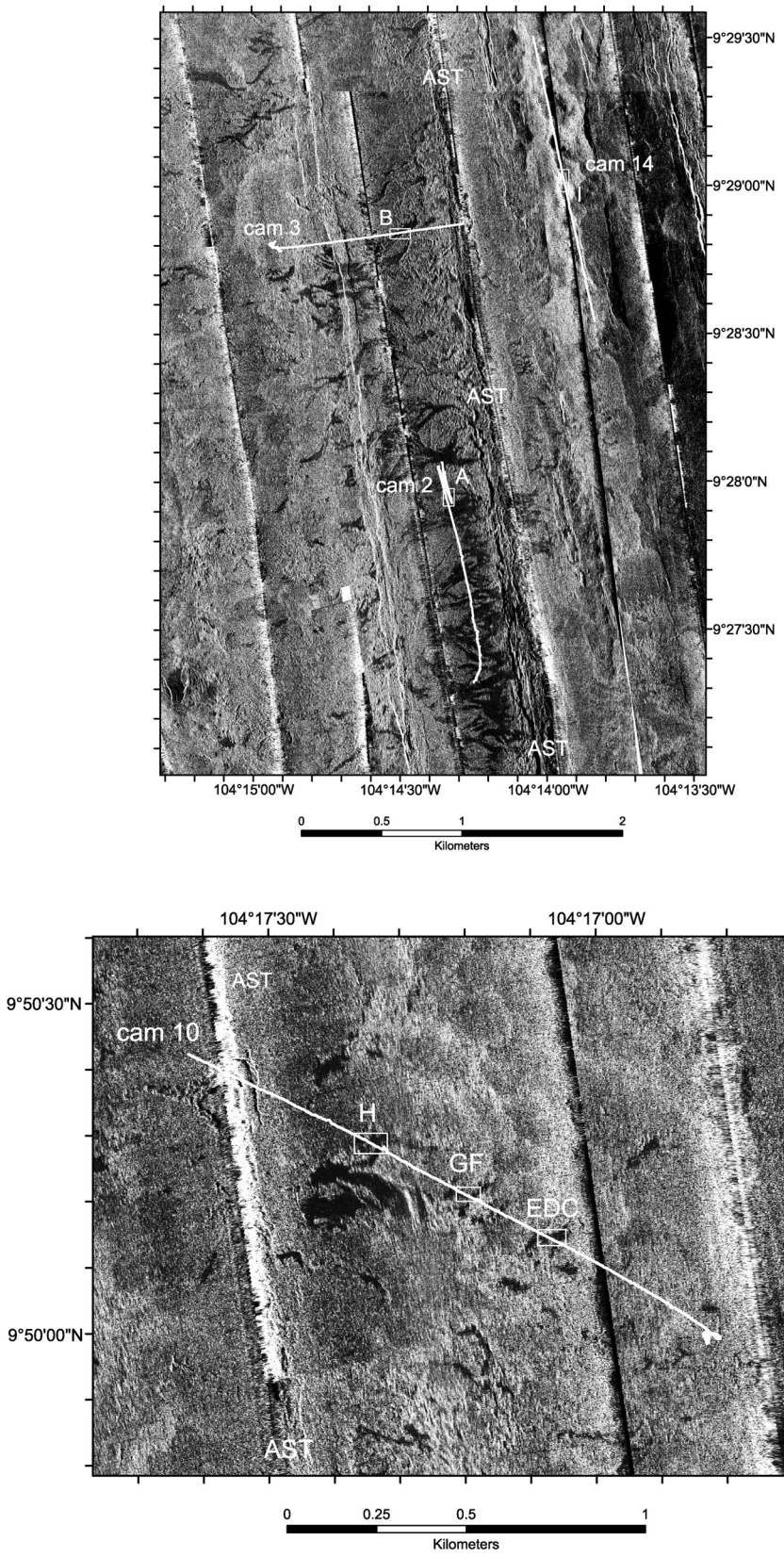

Figure 9. DSL-120 side-scan sonar data of the EPR between 9° and 10°N from cruise AT 07-04. Light areas represent high return, and dark areas represent low return of acoustic reflectivity. White lines mark the path of the camera tows and boxes outline the sections of the traverse covered by the mosaics. Letters indicate the individual submarine channels located within the boxes. The location of the Axial Summit Trough (AST) is indicated.

sheet flow, which comprise 20% of the flow morphology along the AST between 9°49′–52′N, while 66% of the area is lobate lava [*Kurras et al.*, 2000]. Though lava channels are found near the axis, mapping of lava channels [*Kurras et al.*, 2000; *Soule et al.*, 2005] indicates transport of lava 1.5–2.0 km off axis. Camera tow 2 traverses a field of lava channels with a source at the AST (Figures 1 and 9). These channels show a complex bifurcation pattern and extend >0.50 km away from the axis (Figure 9). Channels that initiate off-axis (e.g., Figure 9, channels C, D, E), are short (<0.25 km), narrow channels that do not show a complex bifurcation pattern. See *Soule et al.* [2005] for a detailed discussion of channel distribution in this area.

[22] The scale used for measurements on the digital image mosaics is based on a calibration test that demonstrated an image taken at 5 m altitude covers a 4.8 × 6.4 m (30.7 m^2) section of seafloor [*Fornari*, 2003]. The camera was manually controlled by hauling on the winch to maintain a mean 5 m altitude above the seafloor as determined by returns from a 12 kHz pinger mounted on the camera frame. For reference, a deviation in camera elevation of ±0.5 m during a traverse results in a fluctuation of +7 m^2 to −5 m^2 for area covered by a single image. Our measurements are based on the camera remaining at 5 m above the seafloor, and we have presented associated errors where appropriate. Apparent submarine channel widths are measured across the imaged section of channel from levee to levee and minimum widths are obtained for partial channel maps. Channel dimensions are presented in Table 3. The apparent width of the narrowest channel mapped is 7 m ± 0.7 m while the widest channel is 111 m ± 11 m.

3.3. Surface Textures

[23] In all submarine channels we investigated, the channel interiors contained the same flow textures: smooth, lineated, folded, jumbled, and jigsaw (Figure 3), although in different relative abundances (Figures 8c and 8d).

[24] Smooth crust is flat and featureless, and this texture is commonly sediment-covered within the field area (Figure 3a). Flow surfaces that display high concentrations of closely spaced, relatively flow-parallel ridges and furrows are mapped as lineated (Figure 3b). The ridges vary in width from fine (≤10 cm) to broad (≤50 cm). Closer observations of the ridges show that the width of a single ridge may shrink and swell, as well as combine and divide when traced downstream. A lava coil (Figure 3g) is observed in one of the lineated zones in the channels we analyzed.

[25] It is important to note that the lineated zones described in the channels presented here are fundamentally different from those described by *Chadwick et al.* [1999] on the Juan de Fuca ridge. Channel lineations along the Northern EPR are discrete zones, usually less than tens of meters wide, and reflect elongate, closely spaced, flow-parallel folds bounded by smooth, jumbled, or nonflow

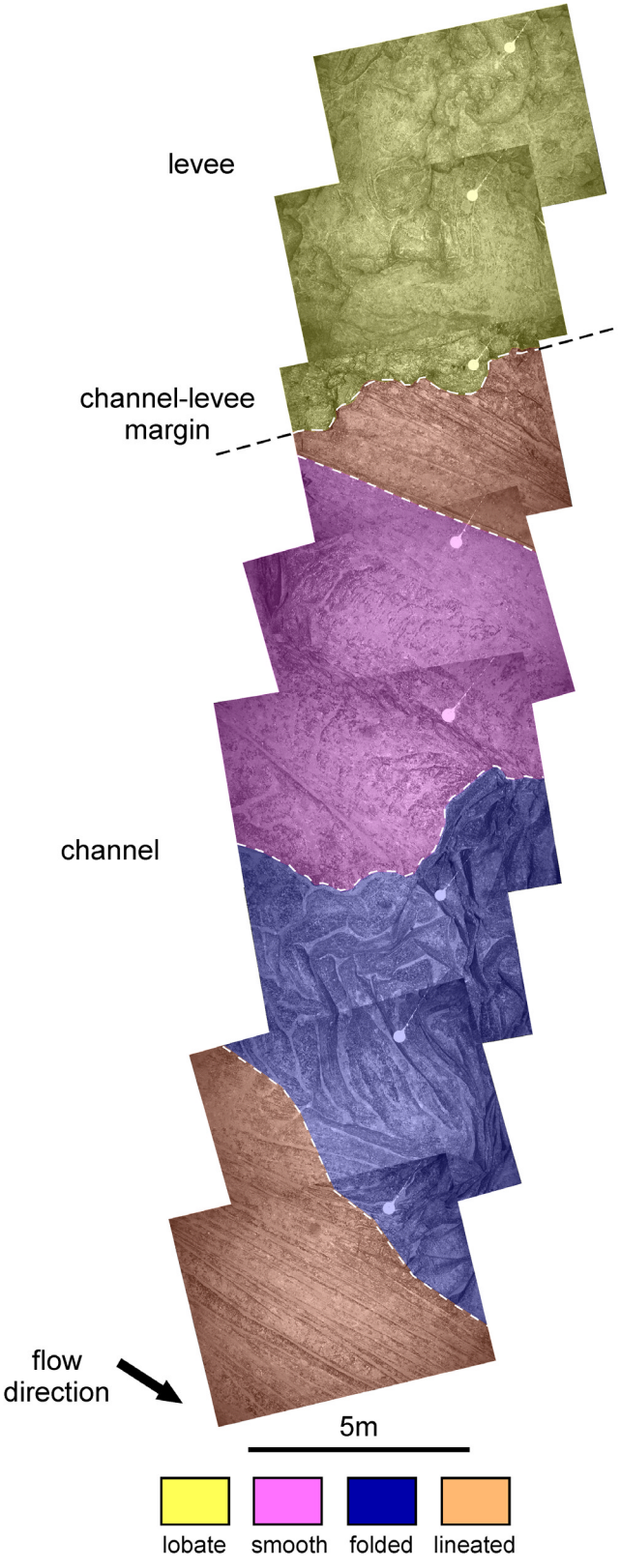

Figure 10. Partial mosaic of channel E from camera tow 10 (location of mosaic is outlined in Figure 11). This section displays folded, lineated, smooth, and lobate crust. Camera tow direction is from bottom to top of page. Dashed lines indicate margin between lobate levee (at top) and channel interior as well as individual textures. Illuminated object in upper right corner of images is a wax "corer" attached to the camera used to collect samples.

Table 3. Dimensions and Texture Coverage for Submarine Lava Channels

		Mosaic Channel Dimensions				Textures							
						Smooth		Lineated		Jumbled		Folded		Jigsaw	
Mosaic	Camera Tow	Width,[a] m	Error[b]	Area,[c] m^2	Error	Area, m^2	Error	Area, m^2	Error	Area, m^2	Error	Area, m^2	Error	Area, m^2	Error
A[d]	2	84	+10/−7	520	+119/−92	297	+68/−52	121	+27/−22	87	+20/−15	0	0	16	±3
B	3	111	±11	741	+161/−137	291	+63/54	142	+31/−26	259	+56/−48	8	+2/−1	41	+9/−8
C	10	10	±1	62	+14/−11	16	±3	16	+4/−3	1	±1	0	0	28	+6/−5
D	10	20	±2	125	+27/−23	72	+16/−13	29	+6/−5	25	±5	0	0	0	0
E	10	57	+5/−6	358	+78/−66	145	+32/−27	122	+26/−22	0	0	58	+13/−11	32	+7/−6
F	10	19	±2	109[e]	+24/−20	33	+7/−6	75	+16/−14	0	0	0	0	1	±0.2
G	10	7	±0.7	42	+9/−8	19	±4	23	+5/−4	0	0	0	0	0	0
H[d]	10	29	±3	205	+45/−38	84	+18/−16	36	+8/−6	85	+18/−16	0	0	0	0
I	14	35	±3	209	+45/−39	112	+24/20	0	0	15	±3	82	+18/−15	0	0

[a]Channel width, apparent channel width measured from levee to levee.
[b]Errors expressed are for variations in elevation of tow camera at 5.5 and 4.5 m from the ocean floor.
[c]Channel area, total area of the channel covered by tow camera images.
[d]Mosaics for channels A and H do not cover the entire channel width. Measurements reflect minimums.
[e]Area does not include estimate regarding missing image. See Figure 11.

parallel folded textures (Figure 10) [*Soule et al.*, 2005]. The compressional fold axis in lineated crust is normal to flow direction. These lineated textures are interpreted to form by a shearing of the crust, a mechanism discussed below. In contrast, the lineated textures discussed by *Chadwick et al.* [1999] extend hundreds of meters along the flow and are characterized by narrow, flow-parallel, corrugated grooves with <5 cm of relief formed by "raking" of solidifying, flowing lava under a broken margin of an overlying crust. We do not refute the model presented by *Chadwick et al.* [1999] but seek to explain the type of lineated submarine texture mapped in the Northern EPR lava channels based on the characteristics we observe and their context within the lava channels.

[26] Folded textures may be "ropy" or "curtain-folded" (Figure 3c). Channel I, for example, has ropy folds that are parabolic, with the nose of the parabola pointing downstream. In contrast, the curtain folds observed in channel E are v-shaped, with the apex of the v pointing upstream. Chaotic regions of coarse, angular chunks of crust are mapped as jumbled (Figure 3d). Folded and lineated textures are commonly observed as closely spaced pieces of crust that fit together like a puzzle. They appear largely undisturbed and to have been connected to nearby coherent sections of channel crust. We refer to this type of disrupted crust as "jigsaw" (Figure 3f).

[27] Lobate crust is characterized by overlapping, bulbous forms, similar to subaerial pahoehoe flows (Figure 3e) and is observed at the margins of the interpreted channels (Figure 5). In most of the submarine channels, the channel crust and levee crust are not attached at the channel-levee margin. This disconnect has been interpreted to represent the draining of lava within the channel and subsequent sagging of the surface crust [*Soule et al.*, 2005].

3.4. Surface Texture Distribution

[28] Maps of the nine submarine lava channels show similar spatial distributions of textures (Figure 11). Specific textures consistently occur at the channel levee margins and within the central part of the channel. Channel interiors tend to be dominated by broad zones of smooth and jumbled crust separated by narrow zones of lineated crust. The lava texture at the channel margins, i.e., immediately adjacent to the lobate levee boundaries, are mainly lineated or jigsaw, although smooth lava and a transitional "jumbled" lava also locally occurs (channels D, H and I in Figure 11) in this region.

[29] Distributed throughout each channel interior are two to three smooth zones of various widths, separated by other textures. These smooth zones are situated off center from the middle of each channel. Only channels C and G (each <10 m wide), and channel H (a partial mosaic)have a single, central smooth zone. Interspersed between zones of smooth crust are narrower zones of lineated crust. Jumbled crust occurs as both broad (e.g., Figure 11, channel B) and narrower zones (e.g., Figure 11, channel D) adjacent to smooth crust. The zones of folded crust imaged in channels B, E, and I are situated off center, away from the channel margins.

[30] Similar to the PEG channels, smooth crust is the most abundant texture observed in submarine lava channels, accounting for 45% of the total submarine crust mapped for

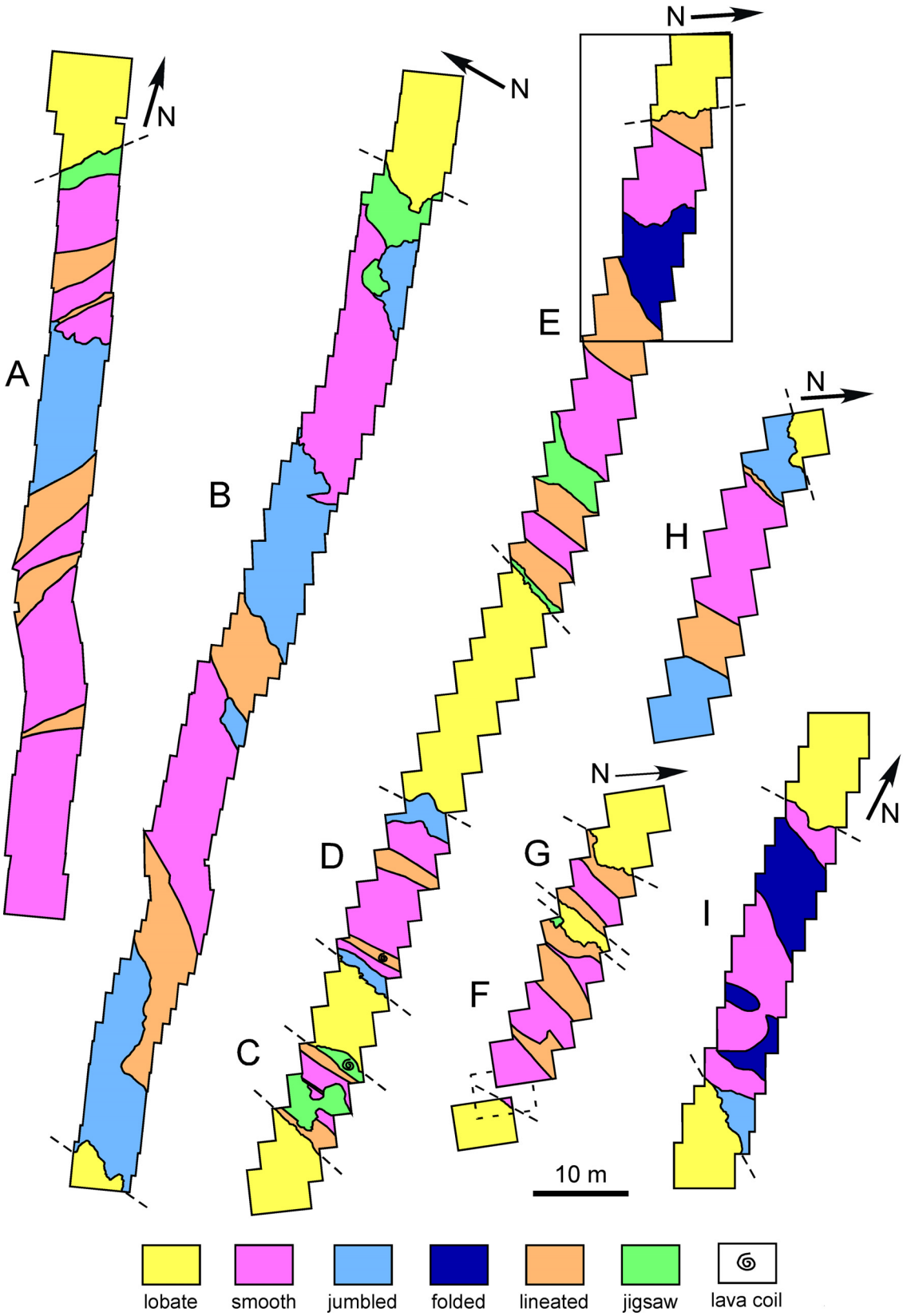

Figure 11. Surface texture maps of submarine lava channels. Flow direction is toward the right for each channel. Dashed lines mark the channel-levee margins for each channel. The maps are not aligned spatially relative to each other and do not represent multiple cross sections of a single channel. Arrows point north in relation to each mosaic. Solid line box outlines portion of mosaic shown in Figure 10. The dashed box in channel F represents a missing image.

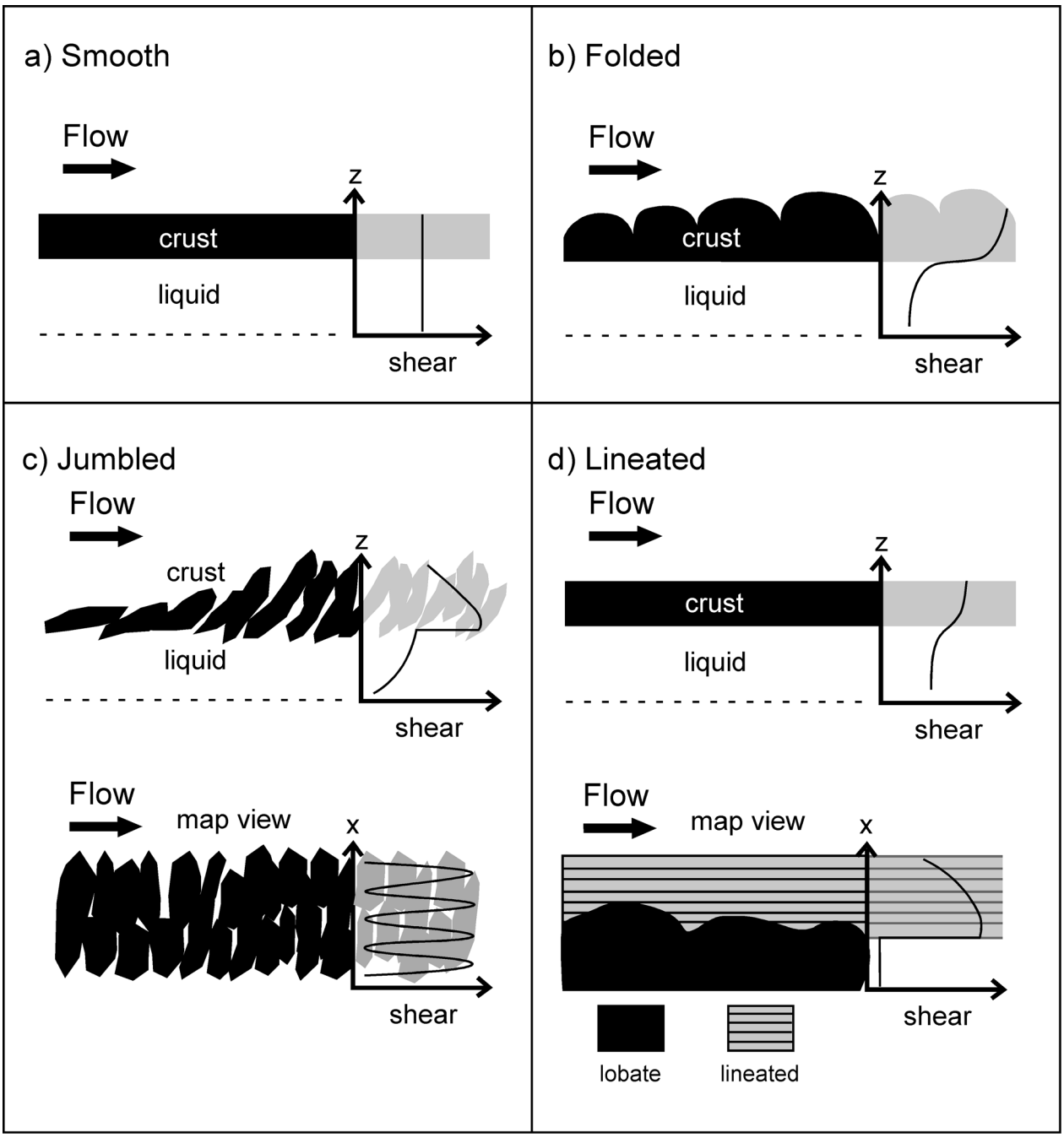

Figure 12. Qualitative shear gradients across the vertical cross-sectional boundary between the surface crust and underlying liquid lava for the formation of each specific textures. A map view is included for jumbled and lineated textures.

this study (Figure 8c). For seven of the channels, smooth crust covers 39–58% of sections imaged (Figure 8d). Folded crust is the least common texture, comprising only 6% of the total mapped area for submarine channels. Narrower channels, <20 m wide, (Figure 8d, channels C, F, G) have a higher percentage of coverage by lineated crust than wider channels (Figure 8d, channels A, B, H, I), with channels D and E as exceptions. The majority of the jigsaw crust we observed was adjacent to lineated and smooth textured crust; all three combined, comprise almost 75% of the textures we mapped in the channels (Figure 8c).

4. Discussion

[31] One of the most difficult aspects of submarine lava flows to recreate in the lab is the highly temperature-dependent rheology of the lava. The low solidification temperature of PEG proves useful in this respect when

compared to other analog materials [e.g., *Fink and Griffiths*, 1990]. Crust in simulated channels can begin to form near (<10 cm) or far (>20 cm) from the vent. Though a crust-free channel may be present in simulated flows (Figure 4a), we do not infer that submarine channels remain crust-free for significant distances from the source. The textures in both environments preserve the processes acting on the crust at the time of solidification, regardless of how far from the source the crust solidifies.

[32] Submarine channels may originate in one or more of the following ways: (1) as an unconfined sheet flow where the slower moving margins solidify, concentrating the flow into a preferred pathway bound by levees, similar to channeled PEG flows [e.g., *Gregg and Fink*, 1995]; (2) localized rapid flow within a lobate flow, disrupting overlying crust and exposing the channel; and (3) confinement within a previous topographic low or channel. Determining the specific origin of the channels we have studied is beyond the scope of this paper and our data, and remains an open question in subaerial lava channels as well. However, the textures contained within the channels we analyzed still reveal a story about their emplacement.

4.1. Formation of Textures

[33] In PEG flows, smooth crust forms near the vent after effusion has ceased. We infer that the crust and underlying liquid wax are moving at the same gravitationally driven flow rate, and that the velocity gradient and shear forces between the coupled components of crust and liquid wax relative to the solidification rate are too low to cause folding of the crust (Figure 12a). In our experimental flows, these conditions were generally met after effusion from the vent had ceased and the liquid wax drains from the channel (Figures 2b, 4c, and 4d), but this does not imply that smooth crust only forms after effusion has ceased. The smooth texture can be formed in a submarine channel under similar conditions, where the shear forces between the overlying channel crust and underlying lava are not high enough to deform the crust (Figure 12a). These conditions can be achieved by a relatively low flow rate in the channel, or in lobate and sheet submarine flows, by the presence of a vapor layer of trapped bubbles of heated seawater that decouples the crust from the lava [*Fornari et al.*, 1998; *Perfit et al.*, 2003]. The vapor layer acts as a buffer between the solidifying crust and underlying lava, negating the velocity and shear gradients between the two components. The vapor layer is not required for the formation of smooth crust in submarine lava channels, but should still be considered as another possible mechanism for reducing the shear gradient between the lava and overlying crust, thereby reducing the chance for crustal deformation.

[34] On the basis of observations of PEG channels [*Griffiths et al.*, 2003], the width of marginal shear zones is proportional to the mean flow velocity in the downflow direction. Observations of subaerial and simulated channels reveal that the highest velocities are near or at the channel center [e.g., *Lipman and Banks*, 1987; *Griffiths et al.*, 2003]. Within the middle of these channels, compression of surface crust in the downflow direction caused by a velocity gradient between liquid lava or liquid PEG and the overlying ductile crust results in buckling (Figure 12b) [e.g., *Fink and Fletcher*, 1978; *Gregg et al.*, 1998; *Griffiths et al.*, 2003]. In the submarine channels we mapped, folded crust was observed toward the central part of the channel (channels B, E, and I in Figure 11). We infer that folded crust in submarine channels forms within zones of higher velocity with respect to other areas across the channel during emplacement [cf. *Gregg and Fink*, 1995, 2000]. Therefore, even with the relatively instantaneous solidification that occurs when lava interacts with ocean water [*Fink and Griffiths*, 1990], the lava remains ductile long enough to fold [e.g., *Engels et al.*, 2003]. Folded crust can brecciate if the strain rate imposed on the crust increases, the crust's ability to deform ductily decreases, or both, resulting in jumbled textures (Figure 12c).

[35] Shear zones that form along the channel-levee margins in subaerial lava channels due to the horizontal gradient in flow velocity are relatively crust-free and more incandescent than the central part of the flow [e.g., *Lipman and Banks*, 1987; *Griffiths et al.*, 2003]. For simulated flows, shear zones are also characterized by a relatively crust-free surface, leaving an exposed gap of liquid PEG between the levee and the channel crust (Figure 6). In a series of PEG experiments, *Griffiths et al.* [2003] observed that the width of shear zones increase while the width of channel crust rafting downstream narrows for higher volume flux and lower cooling rates. We observe relatively crust-free shear zones along the channel-levee margins during emplacement of PEG channels and lineated crust at the same location where the shear zones were present in the final flow morphology (Figures 2 and 4).

[36] The channel-levee margin in a submarine channeled flow is typically an abrupt contact between lobate (levee) and lineated (channel) crust (e.g., Figure 10). We interpret the lobate lavas to form from a relatively slow emplacement and low local velocity in comparison with the more rapidly emplaced lineated flows [cf. *Gregg and Fink*, 1995]. On the basis of comparison with the behavior of subaerial and simulated lava channels [*Lipman and Banks*, 1987; *Gregg and Fink*, 2000; *Griffiths et al.*, 2003], we infer that submarine lineated crust adjacent to lobate levees forms in a shear zone, where rates of shear are comparable to rates of surface solidification (Figure 12d). This is supported by the presence of lava coils (Figures 3f and 11, channel D) within submarine lineated crust, which require a plastic crust and lava flowing at a sufficiently high velocity to rotate the crust before it solidifies [*Lonsdale*, 1977]. Similar features are recognized in subaerial pahoehoe toes [*Gregg and Keszthelyi*, 2004] and again are attributed to high shear rates imposed on partially solidified, yet plastic crust.

[37] Shear zones are not limited to the channel-levee margins, but also can be present within the channel interior. Mapping of submarine channels shows that several zones of smooth crust may form across a single channel and that lineated textures commonly separate these regions from each other (Figure 11, channels A, B, D, H) [*Soule et al.*, 2005]. Given that submarine channels can exceed 100 m in width, it is possible that crust strips, as observed in our PEG simulations, can influence velocity gradients across the channel such that shear zones are not confined only to the channel margin. In PEG simulations, the multiple fold trains appear to reflect a lateral component of flow that imposes a

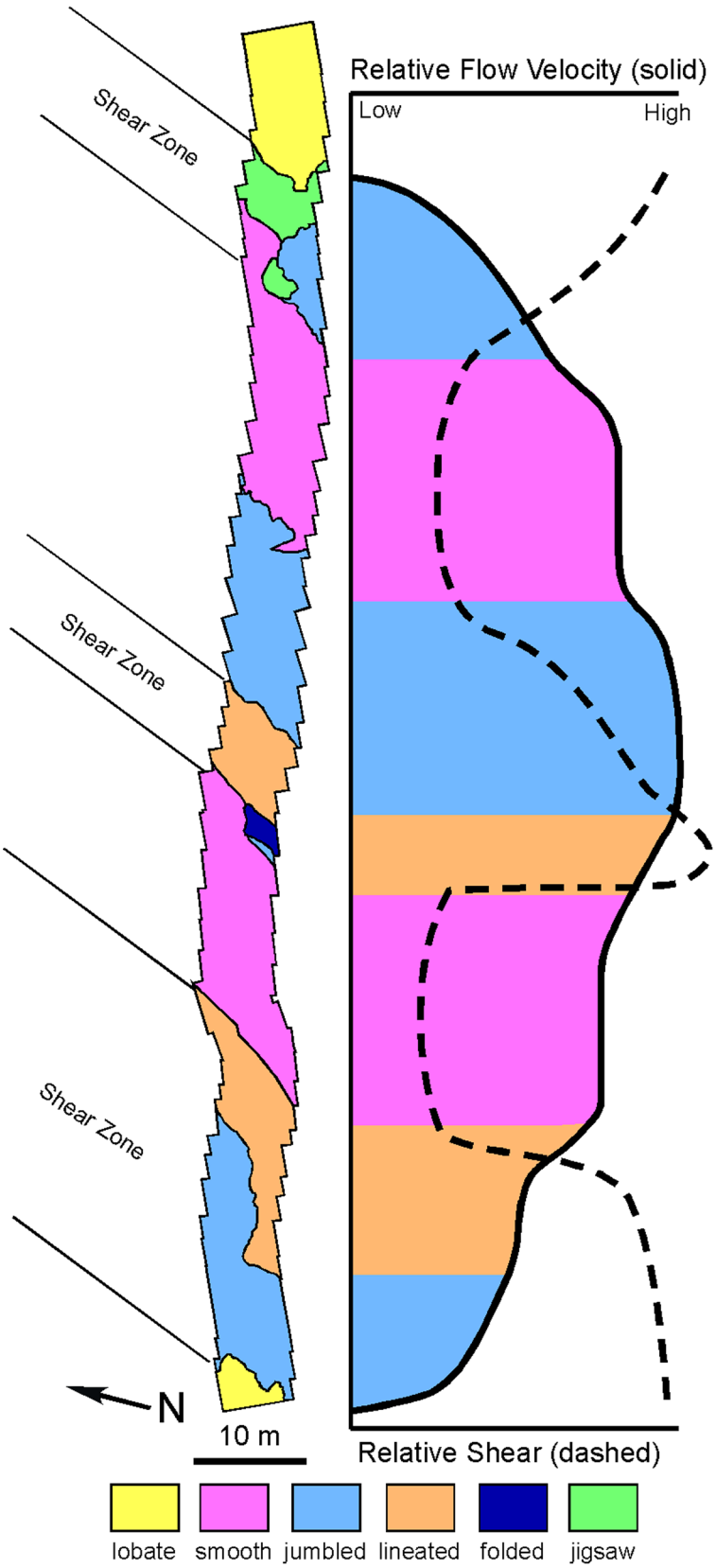

Figure 13. Interpretation of shear zones and relative flow velocity across the channel width of submarine channel B (Figure 11) based on the surface texture locations. The inferred velocity profile is shown by the solid line and shear rate by the dashed line. A brittle zone near the center of the channel is interpreted to be the location of the highest relative flow velocity. Flow direction is to the right. North arrow is shown for context.

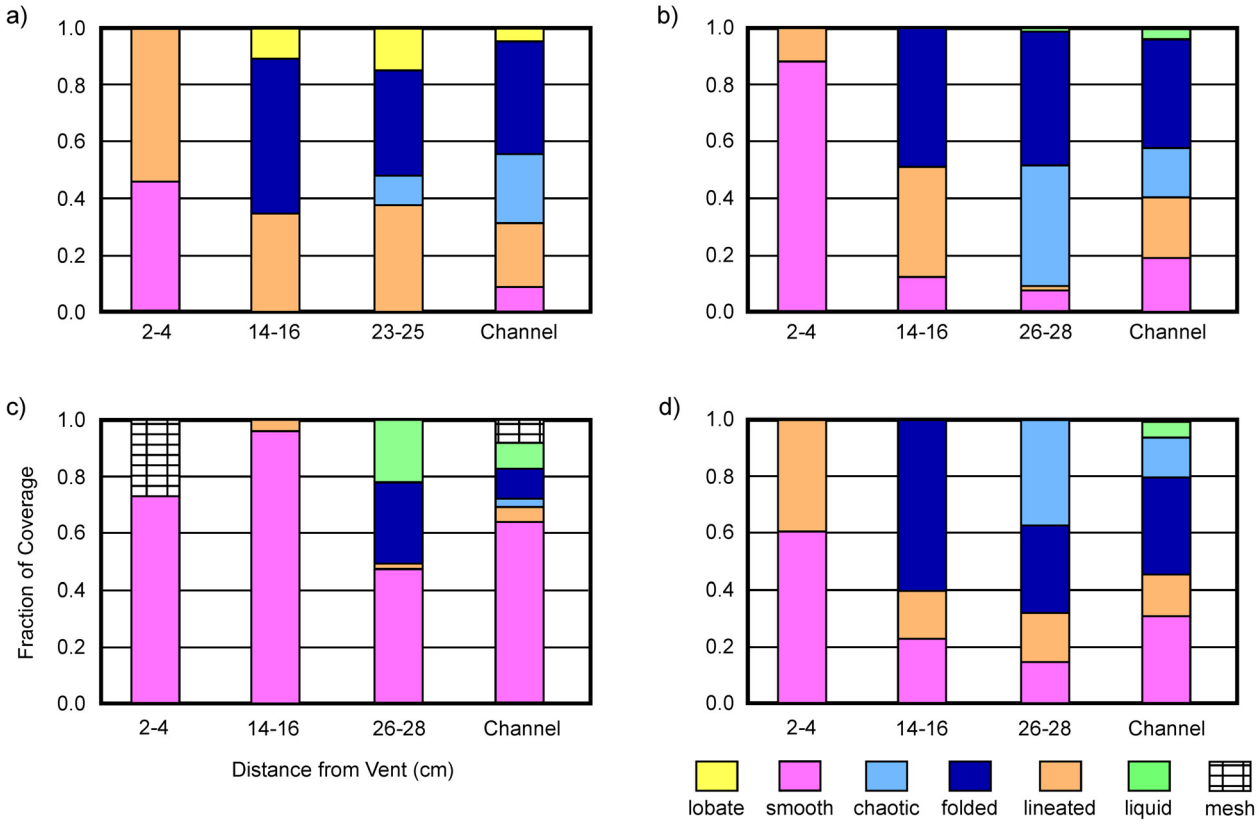

Figure 14. Downstream changes in texture coverage for PEG channels. Fraction of coverage by textures contained within defined sections of the channel spaced at various distances from the vent compared to the total coverage by each texture in the channel excluding the levees. The last column represents the total coverage by all textures in the entire channel. (a) BG-59, (b) BG-63, (c) BG-67, and (d) BG-75.

tension on the crust as it begins to solidify and are typically observed at locations distal from the vent (>20 cm) where both the flow width and channel width have increased. We propose that zones of lineated crust within the submarine channel (e.g., channels A and B in Figure 11) are the result of shear zones that develop between the sections of mobile crust, as observed in PEG channels (Figure 6).

[38] Our interpretation of how textures form allows us to infer emplacement dynamics. Here, we discuss the emplacement of the widest submarine channel we analyzed, channel B (Figure 13). The distribution of smooth textures across the flow suggests that there were at least two areas of relatively constant flow velocity across the channel divided by a centralized zone of lineated and jumbled crust. The zone of smooth crust near the right levee (toward the bottom of the map) is bound on either side by lineated crust and a local patch of folded crust, indicating differences in flow velocity, the presence of shear zones and a ductile response by the crust bordering the smooth crust. This shear zone is ~30 m wide. The zone of smooth crust at the upper portion of the map is bound by jumbled crust, indicating a brittle response to the shearing. On the basis of its appearance, the centralized zone of jumbled crust strongly suggests autobrecciation by high flow velocity and shear between the crust and underlying lava toward the middle of the channel (Figure 13). The flow velocity decreases toward the margins, with zones of relatively equal velocities where smooth crust is present. The distribution of the textures also reveals the differences in cooling and velocity gradients across the flow width. The inferred velocity profile in Figure 13 is a qualitative prediction and its undulating nature differs from the nearly uniform profile across submarine channels predicted in quantitative models [e.g., *Soule et al.*, 2005]. This complex velocity profile (Figure 13) may represent a snapshot in time, the accumulation of different textures as other parts of the channel were active at various times, or transport of crust that was formed at a different portion along the channel.

4.2. Downstream Trends in Texture Coverage

[39] The submarine photo mosaics we collected cover a limited portion of a given channel in contrast to PEG channels, where we can easily observe the entire flow. Therefore interpretations of the flow dynamics across a submarine channel are only applicable to the observed portion of the channel. We have attempted to understand our limited view of submarine channels by surveying texture coverage within selected strips across PEG channels and comparing the results to the entire channel (Figure 14). To characterize the textures distributed within the channel

interior, 2-cm-long strips are placed at distances proximal (2–4 cm), medial (14–16 cm), and distal (>23 cm) from the vent (Figure 5).

[40] Several downstream trends in texture coverage of PEG channels are revealed by this method of analysis. The diversity of textures present in the channel increases with distance from the vent. Smooth crust is prominent proximal to the vent and its abundance decreases downstream; folded crust increases in coverage with distance from the vent. The distal portion of the channel is the most representative of the total coverage by textures in the entire channel.

[41] The complex patterns of textures across submarine channels (Figure 11) resemble the diverse coverage of textures at the distal end of channels in simulated flows (Figure 14). This is logical because the camera tow paths cross the medial and distal ends of the submarine lava channels, the dark areas in the side scan data (Figure 9) represent entire channels. On the basis of this information, we infer that distal sections of submarine channels will show greater diversity in textures across the channel interior, while areas proximal to the source will show less. This diversity can be attributed to complex flow dynamics across the channel or accumulation of textured crust from upstream.

5. Conclusion

[42] Four textures observed in submarine channeled lava flows (smooth, lineated, folded, and jumbled) are also observed in simulated channeled flows in the laboratory. Our interpretations of how these textures form in the submarine environment are based on relationships found in the simulated flows between the processes occurring during effusion and the arrangement of textures in the final flow morphology. Folded crust is formed by a ductile response of the crust to compressional forces in the flow direction, whereas jumbled crust is the disruption of brittle crust due to these forces. Lineated crust, as observed in our field area, is a ductile response of the crust to shearing. Smooth crust is formed when shear and compressional forces are either minimal or nonexistent to deform the crust.

[43] On the basis of the spatial distribution of textures across the channel we can infer velocity gradients across the channel, locations of shear zones, and if the section of channel imaged is relatively proximal, medial, or distal to the source. Our results indicate that surface morphologies within channels reflect the complexities of flow dynamics across a channel during emplacement. Even though texture maps across different submarine channels show similarities, each has its unique characteristics. We conclude that the individual patterns indicate that flow dynamics across each flow is unique and or that the crusts formed at different times and places in the channel system can accumulate at the location of our observations. Further study of submarine channels and additional PEG experiments attempting to simulate specific conditions within channels and at different stages of eruption will help define these relationships.

[44] **Acknowledgments.** We thank Hans Schouten and Maurice Tivey, Co-Chief Scientists of AT7-04, the crew of R/V *Atlantis*, and the National Deep Submergence Facility Operations Group at Woods Hole Oceanographic Institution (WHOI), and the Hawaii Mapping Research Group for exceptional field support during data acquisition and at-sea sonar data processing. The cruise was funded by a grant to WHOI from the National Science Foundation (NSF) OCE-9819261, with additional funding provided by WHOI thorough the Vetlesen Foundation. The PEG experiments were funded by NSF OCE-0425073 in a grant to Tracy Gregg. We extend our thanks to Pete Avery and Gary Nottingham for helping to build the PEG tank and to Tomoko Kurokawa for cataloging the seafloor images at sea.

References

Baker, V. R., G. Komatsu, T. J. Parker, C. V. Gulick, J. S. Kargel, and J. S. Lewis (1992), Channels and valleys on Venus: Preliminary analysis of Magellan data, *J. Geophys. Res.*, *97*, 13,421–13,444.

Blake, S., and B. C. Bruno (2000), Modeling the emplacement of compound lava flows, *Earth Planet. Sci. Lett.*, *184*, 181–197.

Chadwick, W. W., Jr., T. K. P. Gregg, and R. W. Embley (1999), Submarine lineated sheet flows: A unique lava morphology formed on subsiding lava ponds, *Bull. Volcanol.*, *61*, 194–206.

Cormier, M. H., W. B. F. Ryan, A. K. Shah, W. Jin, A. M. Bradley, and D. R. Yoerger (2003), Waxing and waning volcanism along the East Pacific Rise on a millennium time scale, *Geology*, *31*, 633–636.

Dawson, J. B., H. Pinkerton, G. E. Norton, and D. M. Pyle (1990), Physiochemical properties of alkali carbonatite lavas: Data from the 1988 eruption of Oldoinyo Lengai, Tanzania, *Geology*, *18*, 260–263.

Engels, J. L., M. H. Edwards, D. J. Fornari, M. R. Perfit, and J. R. Cann (2003), A new model for submarine volcanic collapse formation, *Geochem. Geophys. Geosyst.*, *4*(9), 1077, doi:10.1029/2002GC000483.

Fink, J. H., and R. C. Fletcher (1978), Ropy pahoehoe; surface folding of a viscous fluid, *J. Volcanol. Geotherm. Res.*, *4*, 151–170.

Fink, J. H., and R. W. Griffiths (1990), Radial spreading of viscous-gravity currents with solidifying crust, *J. Fluid Mech.*, *221*, 485–509.

Fornari, D. J. (2003), A new deep-sea towed digital camera and multi-rock coring system, *Eos Trans. AGU*, *84*, 69, 73.

Fornari, D. J., W. B. F. Ryan, and P. J. Fox (1985), Sea-floor lava fields on the East Pacific Rise, *Geology*, *13*, 413–416.

Fornari, D. J., R. M. Haymon, M. R. Perfit, T. K. P. Gregg, and M. H. Edwards (1998), Axial summit trough of the East Pacific Rise 9°–10°N: Geological characteristics and evolution of the axial zone on fast-spreading mid-ocean ridges, *J. Geophys. Res.*, *103*, 9827–9855.

Fornari, D. J., et al. (2004), Submarine lava flow emplacement at the East Pacific Rise 9°50′N: Implications for uppermost ocean crust stratigraphy and hydrothermal fluid circulation, in *Mid-Ocean Ridges: Hydrothermal Interactions between the Lithosphere and Oceans*, *Geophys. Monogr. Ser.*, vol. 148, edited by C. R. German, J. Lin, and L. M. Parson, pp. 187–218, AGU, Washington, D. C.

Gregg, T. K. P., and W. W. Chadwick (1996), Submarine lava-flow inflation; a model for the formation of lava pillars, *Geology*, *24*, 981–984.

Gregg, T. K. P., and J. H. Fink (1995), Quantification of submarine lava-flow morphology through analog experiments, *Geology*, *23*, 73–76.

Gregg, T. K. P., and J. H. Fink (1996), Quantification of extraterrestrial lava flow effusion rates through laboratory simulations, *J. Geophys. Res.*, *101*, 16,891–16,900.

Gregg, T. K. P., and J. H. Fink (2000), A laboratory investigation into the effects of slope on lava flow morphology, *J. Volcanol. Geotherm. Res.*, *96*, 145–159.

Gregg, T. K. P., and L. P. Keszthelyi (2004), The emplacement of pahoehoe toes: Field observations and comparison to laboratory simulations, *Bull. Volcanol.*, *66*, 381–391.

Gregg, T. K. P., and D. K. Smith (2003), Volcanic investigations of the Puna Ridge, Hawaii: Relations of lava flow morphologies and underlying slopes, *J. Volcanol. Geotherm. Res.*, *126*, 63–77.

Gregg, T. K. P., D. J. Fornari, M. R. Perfit, R. M. Haymon, and J. H. Fink (1996), Rapid emplacement of a mid-ocean ridge lava flow on the East Pacific Rise at 9°46′–51′N, *Earth Planet. Sci. Lett.*, *144*, E1–E7.

Gregg, T. K. P., J. H. Fink, and R. Griffiths (1998), Formation of multiple fold generations on lava flow surfaces: Influence of strain rate, cooling rate, and lava composition, *J. Volcanol. Geotherm. Res.*, *80*, 281–292.

Griffiths, R. W., and J. H. Fink (1992), Solidification and morphology of submarine lavas: A dependence on extrusion rate, *J. Geophys. Res.*, *97*, 19,729–19,737.

Griffiths, R. W., and J. H. Fink (1997), Solidifying Bingham extrusions: A model for the growth of silicic lava domes, *J. Fluid Mech.*, *347*, 13–36.

Griffiths, R. W., K. C. Kerr, and K. V. Cashman (2003), Patterns of solidification in channel flows with surface cooling, *J. Fluid Mech.*, *496*, 33–62.

Harris, A. J. L., L. P. Flynn, O. Matias, W. I. Rose, and J. Cornejo (2004), The evolution of an active silicic lava flow field: An ETM+ perspective, *J. Volcanol. Geotherm. Res.*, *135*, 147–168.

Haymon, R. M., D. J. Fornari, M. H. Edwards, S. Carbotte, D. Wright, and K. C. Macdonald (1991), Hydrothermal vent distribution along the East

Pacific Rise crest (9°09′–54′N) and its relationship to magmatic and tectonic processes on fast spreading mid-ocean ridges, *Earth Planet. Sci. Lett.*, *104*, 513–534.

Hulme, G., and G. Fielder (1977), Effusion rates and rheology of lunar lavas, *Philos. Trans. R. Soc. London, Ser. A*, *285*, 227–234.

Kurras, G. J., D. J. Fornari, and M. H. Edwards (2000), Volcanic morphology of the East Pacific Rise Crest 9°49′–52′N: Implications for emplacement processes at fast-spreading mid-ocean ridges, *Mar. Geophys. Res.*, *21*, 23–41.

Lipman, P. W., and N. G. Banks (1987), Aa flow dynamics, Mauna Loa 1984, in *Volcanism in Hawaii*, vol. 2, edited by R. W. Decker, T. L. Wright, and P. H. Stauffer, *U.S. Geol. Surv. Prof. Pap.*, *1350*, 1527–1567.

Lonsdale, P. (1977), Abyssal pahoehoe with lava coils at the Galapagos rift, *Geology*, *5*, 147–152.

Macdonald, G. A. (1953), Pahoehoe, aa, and block lava, *Am. J. Sci.*, *251*, 169–191.

Mouginis-Mark, P. J., L. Wilson, and M. T. Zuber (1992), The physical volcanology of Mars, in *Mars*, edited by H. H. Kieffer et al., pp. 424–452, Univ. of Ariz. Press, Tucson.

Perfit, M. R., and W. W. Chadwick Jr. (1998), Magmatism at mid-ocean ridges: Constraints from volcanological and geochemical investigations, in *Faulting and Magmatism at Mid-Ocean Ridges*, *Geophys. Monogr. Ser.*, vol. 106, edited by W. R. Buck et al., pp. 59–116, AGU, Washington, D. C.

Perfit, M., J. R. Cann, D. J. Fornari, J. Engels, D. K. Smith, W. I. Ridley, and M. H. Edwards (2003), Interaction of sea water and lava during submarine eruptions at mid-ocean ridges, *Nature*, *426*, 62–65.

Sakimoto, S. E. H., and T. K. P. Gregg (2001), Channeled flow: Analytic solutions, laboratory experiments, and applications to lava flows, *J. Geophys. Res.*, *106*, 8629–8644.

Scheirer, D. S., D. J. Fornari, S. E. Humphris, and S. Lerner (2000), High-resolution seafloor mapping using the DSL-120 sonar system: Quantitative assessment of sidescan and phase-bathymetry data from the Lucky Strike segment of the Mid-Atlantic Ridge, *Mar. Geophys. Res.*, *21*, 121–142.

Schouten, H., M. Tivey, D. Fornari, D. Yoerger, A. Bradley, M. Edwards, and P. Johnson (2002), Near-bottom investigation of the Central Anomaly Magnetic High (CAMH) at the East Pacific Rise 9°25′–57′N, R/V *Atlantis*, Voyage 7 Leg 4, WHOI cruise report, Woods Hole Oceanogr. Inst., Woods Hole, Mass. (Available at http://www.whoi.edu/atlantis74/)

Smith, D. K., and J. R. Cann (1999), Constructing the upper crust of the Mid-Atlantic Ridge: A reinterpretation based on the Puna Ridge, Kilauea Volcano, *J. Geophys. Res.*, *104*, 25,379–25,399.

Soule, S. A., D. J. Fornari, M. R. Perfit, M. A. Tivey, W. I. Ridley, and H. Schouten (2005), Channelized lava flows at the East Pacific Rise crest 9°–10°N: The importance of off-axis lava transport in developing the architecture of young oceanic crust, *Geochem. Geophys. Geosyst.*, *6*, Q08005, doi:10.1029/2005GC000912.

White, S. M., K. C. Macdonald, and R. M. Haymon (2000), Basaltic lava domes, lava lakes, and volcanic segmentation of the southern East Pacific Rise, *J. Geophys. Res.*, *105*, 23,519–23,536.

White, S. M., R. M. Haymon, D. J. Fornari, M. R. Perfit, and K. C. Macdonald (2002), Correlation between volcanic and tectonic segmentation of fast-spreading ridges: Evidence from volcanic structures and lava flow morphology on the East Pacific Rise at 9°–10°N, *J. Geophys. Res.*, *107*(B8), 2173, doi:10.1029/2001JB000571.

Williams, D., R. Greeley, R. M. C. Lopes, and A. G. Davies (2001), Evaluation of sulfur flow emplacement on Io from Galileo data and numerical modeling, *J. Geophys. Res.*, *106*, 33,161–33,174.

Yoerger, D. R., A. Bradley, B. Walden, H. Singh, and R. Bachmayer (1998), Surveying a subsea lava flow using the Autonomous Benthic Explorer (ABE), *Int. J. Syst. Sci.*, *29*, 1031–1044.

D. J. Fornari and S. A. Soule, Woods Hole Oceanographic Institution, Department of Geology and Geophysics, Woods Hole, MA 02543, USA.

W. B. Garry and T. K. P. Gregg, Department of Geology, 876 Natural Science Complex, State University of New York at Buffalo, Buffalo, NY 14260, USA. (brentgarry@yahoo.com)